

Review

# Architectures and Mechanisms of Perylene Diimide-Based Optical Chemosensors for pH Probing

Shuai Chen <sup>1,2,\*</sup> , Meng Zhou <sup>1</sup>, Ling Zhu <sup>1</sup>, Xiaomei Yang <sup>3</sup> and Ling Zang <sup>3,4,\*</sup> 

<sup>1</sup> Jiangxi Key Laboratory of Flexible Electronics and School of Pharmacy, Jiangxi Science & Technology Normal University, Nanchang 330013, China

<sup>2</sup> Jiangxi Provincial Engineering Research Center for Waterborne Coatings, Nanchang 330013, China

<sup>3</sup> Nano Institute of Utah, University of Utah, Salt Lake City, UT 84112, USA

<sup>4</sup> Department of Materials Science and Engineering, University of Utah, Salt Lake City, UT 84112, USA

\* Correspondence: shuaichen@jxstnu.edu.cn (S.C.); lzang@eng.utah.edu (L.Z.);

Tel.: +1-801-587-1551 (L.Z.); Fax: +1-801-581-4816 (L.Z.)

**Abstract:** The precise control and monitoring of pH values remain critical for many chemical, physiological and biological processes. Perylene diimide (PDI)-based molecules and materials exhibit excellent thermal, chemical and photochemical stability, unique UV-vis absorption and fluorescent emission properties, low cytotoxicity, as well as intrinsic electron-withdrawing (n-type semiconductor) nature and impressive molecular assembly capability. These features combined enable promising applications of PDIs in chemosensors via optical signal modulations (e.g., fluorescent or colorimetric). One of the typical applications lies in the probing of pH under various conditions, which in turn helps monitor the extracellular (environmental) and intracellular pH change and pH-relying molecular recognition of inorganic or organic ions, as well as biological species, and so on. In this review, we give a special overview of the recent progress in PDI-based optical chemosensors for pH probing in various aqueous and binary water–organic media. Specific emphasis will be given to the key design roles of sensing materials regarding the architectures and the corresponding sensing mechanisms for a sensitive and selective pH response. The molecular design of PDIs and structural optimization of their assemblies in order to be suitable for sensing various pH ranges as applied in diverse scenarios will be discussed in detail. Moreover, the future perspective will be discussed, focusing on the current key challenges of PDI-based chemosensors in pH monitoring and the potential approach of new research, which may help address the challenges.

**Keywords:** perylene diimide; chemosensor; pH probing; bioimaging; colorimetric sensor; fluorescent sensor



**Citation:** Chen, S.; Zhou, M.; Zhu, L.; Yang, X.; Zang, L. Architectures and Mechanisms of Perylene Diimide-Based Optical Chemosensors for pH Probing. *Chemosensors* **2023**, *11*, 293. <https://doi.org/10.3390/chemosensors11050293>

Academic Editor: Jose M. Pedrosa

Received: 14 April 2023

Revised: 6 May 2023

Accepted: 13 May 2023

Published: 14 May 2023



**Copyright:** © 2023 by the authors. Licensee MDPI, Basel, Switzerland. This article is an open access article distributed under the terms and conditions of the Creative Commons Attribution (CC BY) license (<https://creativecommons.org/licenses/by/4.0/>).

## 1. Introduction

The molecules of perylene 3,4,9,10-tetracarboxyl diimide (PTCDI or PDI) form a series of unique functional semiconductors and conjugated organic dyes or pigments. PDIs have exceptional photo absorption and emission characteristics, excellent thermal, chemical, optical and photochemical stability, as well as outstanding n-type (strong electron affinity) semiconductor properties. These features can be tuned via molecular structure modification, molecular assembly or aggregation, or exogenous chemical action, etc. [1–4]. Such structural and property tunability makes PDIs ideal candidates for development as chemosensors for detection of various chemicals in both liquid and gas phases, especially organic and inorganic ions, and biological species [3,5–8]. Very often, the sensitivity and selectivity of the chemosensors are dependent on the pH of the analyte solution, meaning that monitoring and control of the pH are crucial for precise detection of target analytes. Such pH dependence of sensing performance has been reported and reviewed in some previous publications [3,7,8]. Nonetheless, there is a lack of systematic review of quick and precise detection of the pH value itself with PDI-based optical sensors, although such pH

probing would be crucial for practical application in the health, pharmaceutical, biological, food and environmental analysis scenarios, wherein the pH may change frequently under various conditions. In 2020, Borisov et al. gave an excellent and quite comprehensive review of optical pH sensors, including a brief introduction of PDI sensors for pH probing [9]. In 2021, Singh et al. summarized the progress in PDI-based chemosensors, describing briefly their application in the detection of  $H^+$  and  $OH^-$  ions (equivalent of pH) [8].

Compared to the most popular and widely used commercial pH glass electrodes based on the electrochemical principle, the use of optical (colorimetric, fluorescent) chemosensors removes the technical limits due to expensive, complex and bulky electrical equipment, which usually requires sophisticated control and maintenance [9,10]. Optical sensors can also be visualizable but inert and robust to the interference of extraneous electrical, magnetic and microwave fields. These sensors are more cost effective and could even be used in disposable form, just as the widely used pH test papers, despite some limitation in continuous real-time measurement [10]. Moreover, the small size and aqueous solubility of chromophore and fluorophore make them attractive for use in cell and other biofluid (e.g., blood, urine, etc.) imaging, where it is difficult or impossible to employ pH electrodes. Thus, molecular colorimetric and fluorescent sensors have been recognized as the most competitive techniques for pH probing beyond the conventional pH glass electrodes [9].

The performance of optical sensors as applied in pH probing relies on the sensing mechanisms in association with the structure and property of the sensor materials, which in turn affect the selectivity, sensitivity, response time, dynamic range, reproducibility and temperature dependence of sensing response. In general, the sensing response of pH probing is based on the protonation induced by binding of  $H^+$  ions (protons). The electron-accepting characteristic of PDI skeleton arises mainly from the electron-withdrawing imide groups. Upon functionalization with protonatable electron-donating groups, such as amines, the photoinduced electron transfer (PET) from the amine to the PDI can be modulated by protonation at the amine moiety, thus leading to a sensing response toward protons. Compared to other sensor molecules or materials, PDIs also exhibit good permeability, low cytotoxicity and impressive molecular assembly capability, depending on the rigid polycyclic aromatic core. As a result, PDI sensors have been widely explored for probing extracellular (environmental) and intracellular pH values and pH-relying molecular recognition of inorganic or organic ions, as well as biological species, and so on. Therefore, the main challenges and endeavors undertaken in the past lie mostly in the structural modification and optimization of PDI molecules, especially the side groups, in order to improve their water solubility [5,11].

Considering the increased interest and potential in pH probing enabled by PDI-based optical chemosensors, it is imperative to provide a comprehensive overview of the recent development of colorimetric and fluorescent sensors based on PDI molecules and materials, which can afford effective pH probing for environmental, biofluid or intracellular systems, as presented in this review, with specific focus on the structural and architectural design of sensor materials in correlation with the various sensing response mechanisms (Figure 1). It is our hope that this review will help enlighten the molecular design of novel pH probes, or of the opposite pH-inert probes for metal ions, which will provide effective detection of metal ions with minimal interference of pH fluctuation. We also expect to inspire more explorative research of PDI sensors, which can be applied in biological or even wearable systems, wherein organic sensors are normally more suitable than inorganic counterparts considering the higher flexibility and more options for structural modification of organic materials.

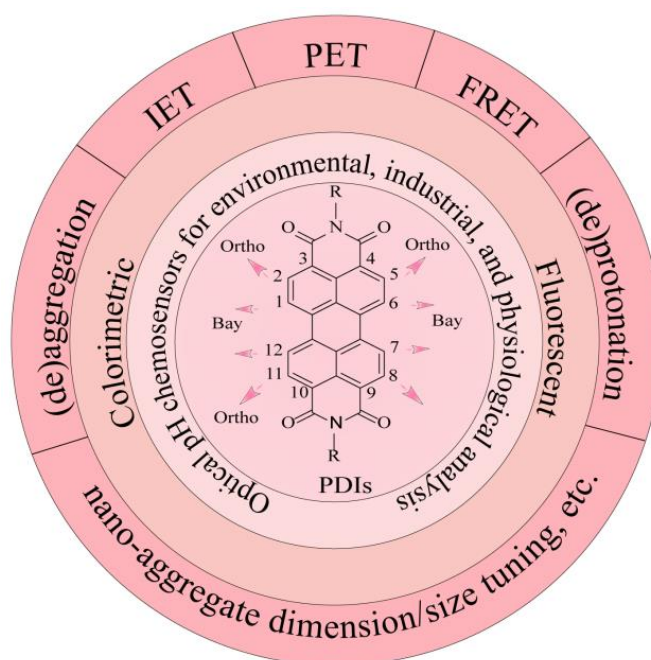


**Figure 1.** Scheme of the design and application of PDI-based colorimetric and fluorescent chemosensors for pH probing.

## 2. Colorimetric Chemosensors

The colorimetric pH response of PDI-based chemosensors benefits from their strong absorptivity in the mid-visible spectral region, with molar absorption coefficient as high as  $30,000\text{--}90,000\text{ cm}^{-1}\text{ M}^{-1}$  [2,10] in the broad spectra (color) variation range [5]. However, due to the rigid perylene skeleton and the unique  $\pi$ -conjugation with the imide nitrogen as the node, structural substitution at the imide position generally has little influence on the spectral absorption property of PDI molecules [1]. At present, only few studies have been reported, such as those on hydrochromism [11] and pH-mediated color change [12], in this aspect, mainly due to the considerable challenge of the intense red background and poor water solubility of hydrophobic PDI core. Satisfyingly, modification at its bay area could result in considerable influence on its absorption spectra and improvement in solubility [1].

### 2.1. Hydrochromism for pH and Humidity Sensing

Upon functionalization of PDI scaffold at its 1,7-bay position by electron-donating 3-hydroxycyclobutenedione moieties, the derivative (namely PDI-1) thus obtained showed pronounced acidity and solubility in polar solvents [11]. The intramolecular electron transfer (IET) between cyclobutene moiety and PDI backbone can be modulated significantly by the protonation/deprotonation of the -OH groups (Figure 2a), thus resulting in bathochromic shift of the absorption peak from 570 nm (acidic form itself) to 612–667 nm (conjugate base form PDI-1<sup>2-</sup> in different organic solvents), as shown in Figure 2b,c. The solvent effect of the colorimetric response can also be utilized for probing the solvent polarity and humidity, which can be applied in monitoring trace water in organic solvents, such as tetrahydrofuran (THF), as well as film sensing of humidity in the gas phase. As shown in Figure 2d, the sensor film, fabricated by immobilization of PDI-1 in polyethylene glycol (PEG) matrix, showed drastic color change from red-purple to blue-green accompanied by distinct absorption spectra change upon exposure to water moisture. Such halochromic response is instantaneous, and reversible, for which the sensor material can be regenerated after drying.

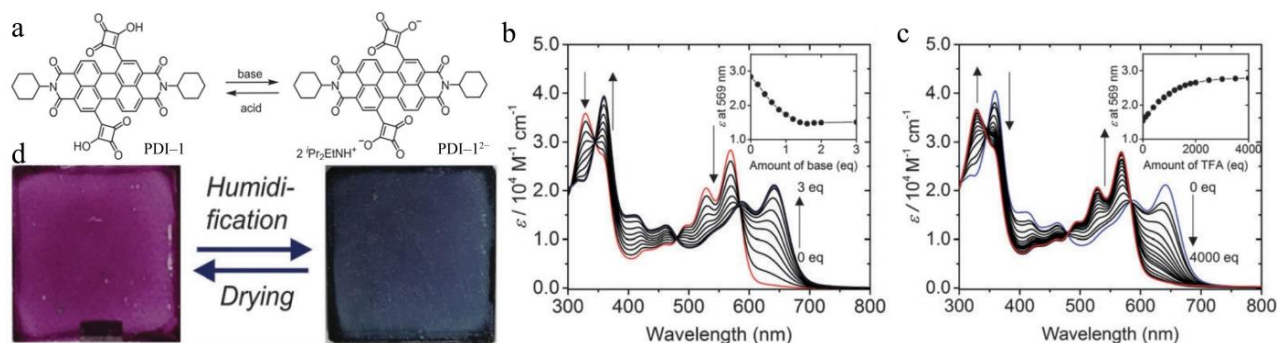


**Figure 2.** (a) Scheme of the molecular structure interconversion of PDI-1 and PDI-1<sup>2-</sup>; The change of absorption spectra of PDI-1 upon addition of (b) diisopropylethylamine (base) and (c) subsequent addition of trifluoroacetic acid (TFA); (d) Photos of the reversible color change of PDI-1 in PEG matrix. Reproduced with permission from Ref. [11].

## 2.2. Synergistic CO<sub>2</sub> and pH Sensing

Similar to the solid-state sensing described above, a PDI molecule substituted at the bay area with the 2-phenylimidazole group, namely PDI-2 (Figure 3), was developed into a CO<sub>2</sub> sensor through the colorimetric response toward pH change [12]. As shown in Figure 3a, the solid-state CO<sub>2</sub> sensor was fabricated by blending PDI-2 with tetrabutylammonium hydroxide (TOA) as the lipophilic base, tributyl phosphate (TBP) as the plasticizer and ethyl cellulose (EC) as the matrix into hydrophilic poly(ethylene terephthalate) as the support. In its pristine state under nitrogen, PDI-2 exists in the deprotonated format by forming a salt with TOA ions, exhibiting a blue color. Upon a decrease in pH, PDI-2 becomes protonated at the imidazole moiety, thus changing its color to red. Such pH response can be adapted to the sensing of CO<sub>2</sub> (Figure 3b), which is a typical weak acid when dissolved in water. By measuring the colorimetric response of the PDI-2 composite sensor immersed in water, the gas phase CO<sub>2</sub> in contact with water can be monitored in a broad pressure range from 0.5 to 1000 hPa. Taking advantage of the structure and composition tunability, the composite sensor of PDI-2 may find wide application in quality inspection of beverage and food packaging, health monitoring and others, where constant monitoring of the pH or CO<sub>2</sub> level is crucial.

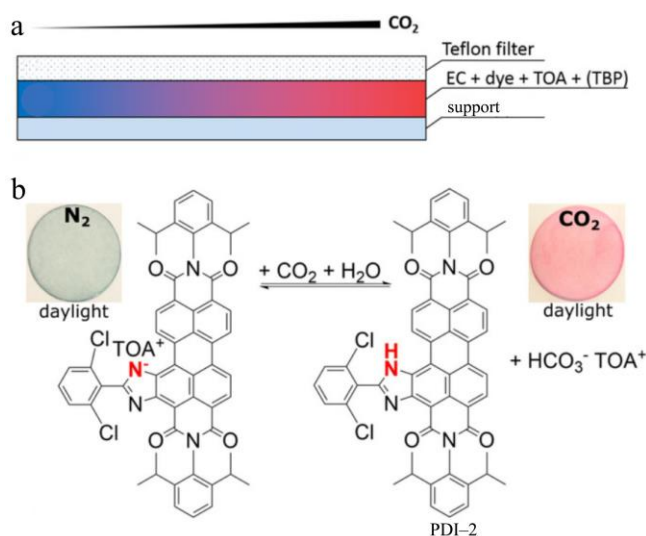


**Figure 3.** (a) Schematic architecture of the solid-state sensor incorporating PDI-2 as a dye used for probing CO<sub>2</sub>; (b) Photographs of the sensor strip recorded under daylight before and after exposure to 100% CO<sub>2</sub>; The colorimetric sensing mechanism based on protonation/deprotonation process mediated by CO<sub>2</sub> is also shown. Reproduced with permission from Ref. [12].

### 3. Fluorescent Chemosensors

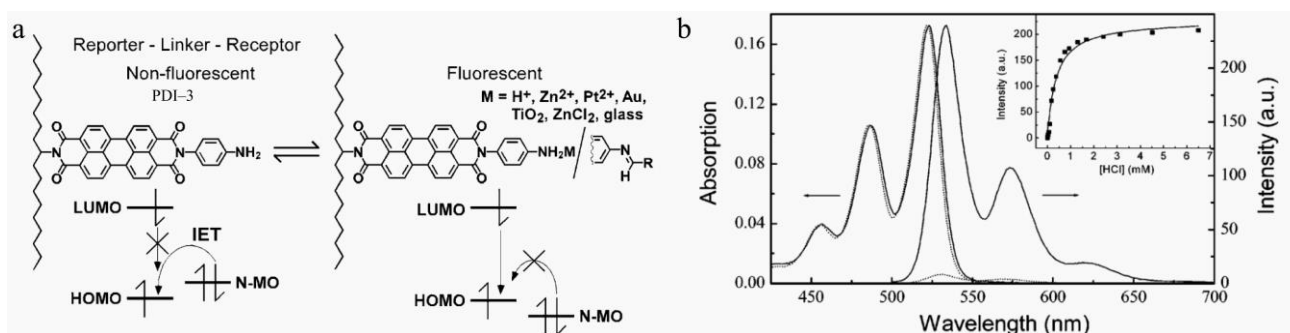
In comparison to the colorimetric sensors (including the most commonly used pH test paper), fluorometric pH probing has intrinsic advantages of fluorophores and the corresponding sensing mechanisms, such as high sensitivity, rapid response and much improved selectivity enabled by the specific molecular design [9,13]. Unlike other common pH-responsive fluorophores, PDIs have been considered as some of the most attractive candidates in chemosensor design because of their excellent electron-accepting ability, strong fluorescence emission (high quantum yield, close to 100% in the monomeric and small oligomeric states) and high photostability [3,4,10]. In general, a PDI-based pH sensor consists of PDI backbone modified with an electron donor group, such as amine, which can interact with protons to initiate the protonation/deprotonation process. Before protonation, the free base state of amines functions as an effective electron donor, causing quenching of the fluorescence of PDI through PET [8,14]. Upon protonation, the energy level of the lone pair of electrons in amine becomes lower than the highest occupied molecular orbital (HOMO) of PDI, thus blocking the PET for PDI. As a result, the strong fluorescence of PDI is resumed. Such fluorescence turn-on response can be utilized to quantize the concentration of protons, as well as probe the change of pH. The substitution with amine in PDI can be either at the imide position or the bay area, and the amine substituents can be primary, secondary, tertiary or aromatic amines. Depending on the substitution position and the type of amines, the fluorescence color (wavelength) and intensity modulation efficiency upon protonation could vary significantly. Since the nitrogen at the imide position is a node in the  $\pi$ -conjugation of PDI, substitution at this position does not change the electronic property of PDIs [1].

As shown in Figure 2, deprotonation of the -OH group generates an anionic state of the cyclobutene moiety, thus increasing its electron-donating power. This results in significant red shift of the absorption peak due to the enhancement of the IET transition [11]. The increased electron-donating power would also enhance the PET process, and thus, fluorescence quenching [8]. For the PDIs without or with minimal bay substitution, the limited solubility in some solvents often leads to molecular assembly (aggregation) primarily driven by the strong  $\pi$ - $\pi$  stacking interaction, resulting in significant quenching of fluorescence [1]. To mitigate the aggregation induced fluorescence quenching, the substitution at the imide or bay area is often modified with steric groups, so as to enhance the molecular dispersion of PDIs in solution [2]. If the substituents are protonatable or deprotonatable, the molecular assembly may become significantly dependent on the pH, which in turn changes the electrostatic interaction between molecules. Depending on the molecular structure design, pH-triggered fluorescence response could be due to various chemistry processes, such as PET [10,12–15], supramolecular (de)aggregation [16,17], fluorescence resonance energy transfer (FRET) [18], tunable lateral dimension of one-dimensional (1D) nanostructure [19] or volume phase transition of unimolecular micelle [20], and so on. These optical pH chemosensors have been intensively utilized for environmental or health analyses and cell imaging [21–23], etc. In addition to fluorescence emission intensity, fluorescence lifetime can also be used as a sensing signal given the excellent photochemical stability of PDIs [24,25].

#### 3.1. pH Sensing Based on Photoinduced Electron Transfer (PET) Mechanism

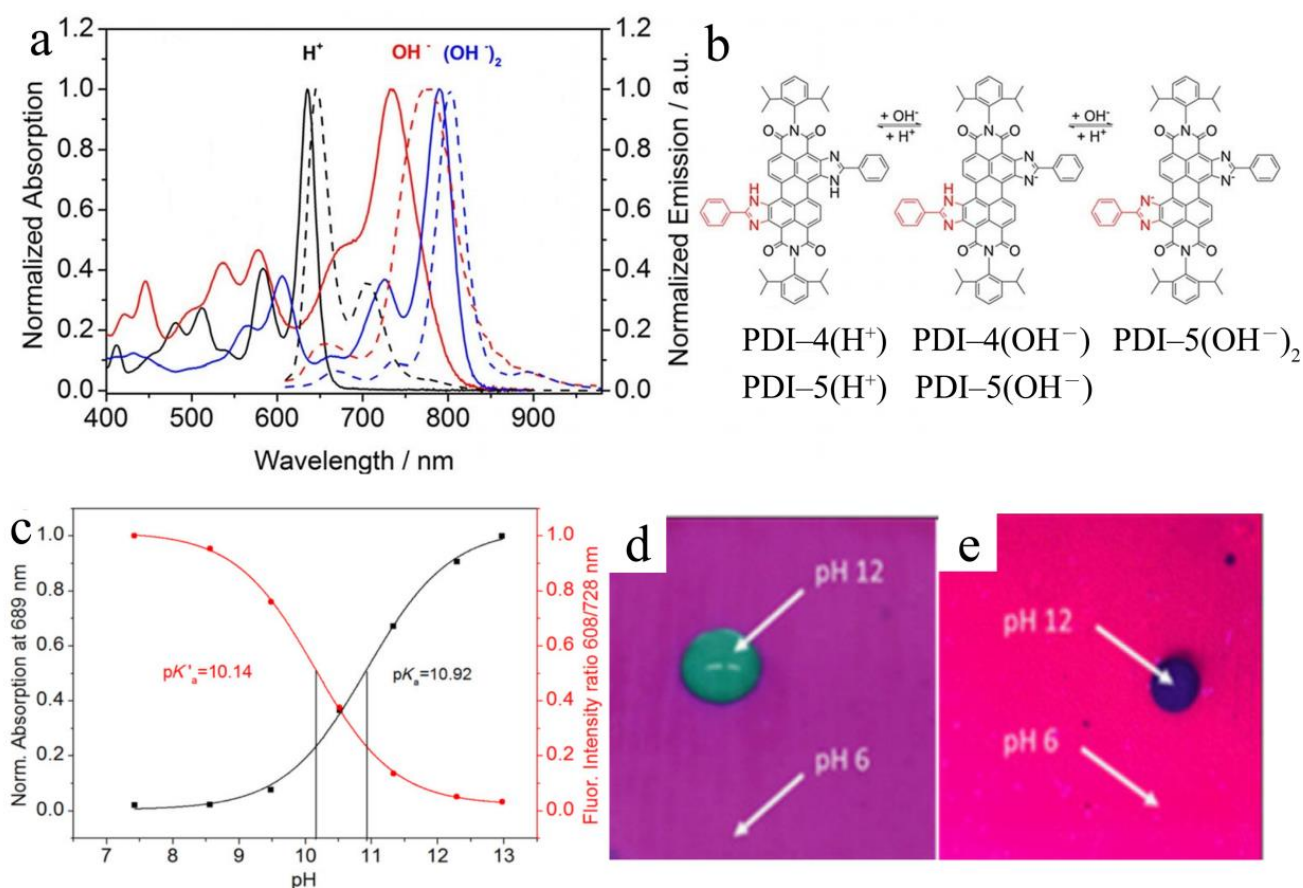
As discussed above, PDI-based pH sensors are commonly reliant on the PET mechanism, for which the electron transfer process occurs between the PDI backbone and electron donor group covalently modified at the imide or bay positions, and the pH response is due to the protonation or deprotonation of the electron donor moiety [14,26]. Despite the highly efficient PET sensing response, PDI fluorescent sensors have been much less used in aqueous media for pH probing in comparison to the more common applications in organic or mixed media for detection of other ionic species [3]. This is likely due to the challenge in tuning the aqueous solubility of PDIs in a wide range of pH. One of the early PDI-based pH sensors, namely PDI-3 (Figure 4a), was composed of an asymmetric structure with

one imide modified with nonyldecyl and the other with aniline [14]. The aniline acts as an electron donor and organic base, which can be protonated, and the nonyldecyl substitution helps prevent molecular aggregation due to the bulky steric hindrance. Thanks to the high molecular dispersibility, PDI-3 was successfully developed as a single-molecule probe for pH, metal ions and other organic functional groups, such as ketone, on surface via protonation and other reactions at the aniline site (Figure 4a) [14]. In the unbound state, the energy level of free base aniline is higher than the HOMO of PDI, and the efficient PET process causes almost complete fluorescence quenching of PDI, resulting in zero emission background. Upon protonation, the energy level of aniline is lowered, thus blocking the PET process. As a result, the fluorescence of PDI is resumed depending on the yield of protonation, which in turn depends on the concentration of protons (or pH), as shown in Figure 4b. However, such fluorescence turn-on sensing response can also be realized through other chemical reactions of aniline, such as coordination interaction with metal ions, such as  $Zn^{2+}$ ,  $Pt^{2+}$ , or Schiff's base reaction with ketones or aldehydes. This poses a challenge for detection selectivity when used in the bulk solution phase, although the different bounding interactions can potentially be distinguished at single-molecule level on the surface by measuring the different "blinking" kinetics of fluorescence [14]. Taking advantage of the quick reversible protonation/deprotonation of amines, PDI sensors based on the PET mechanism have become increasingly popular for pH probing depending on the  $pK_a$  of the amine moieties [10–15,26,27].



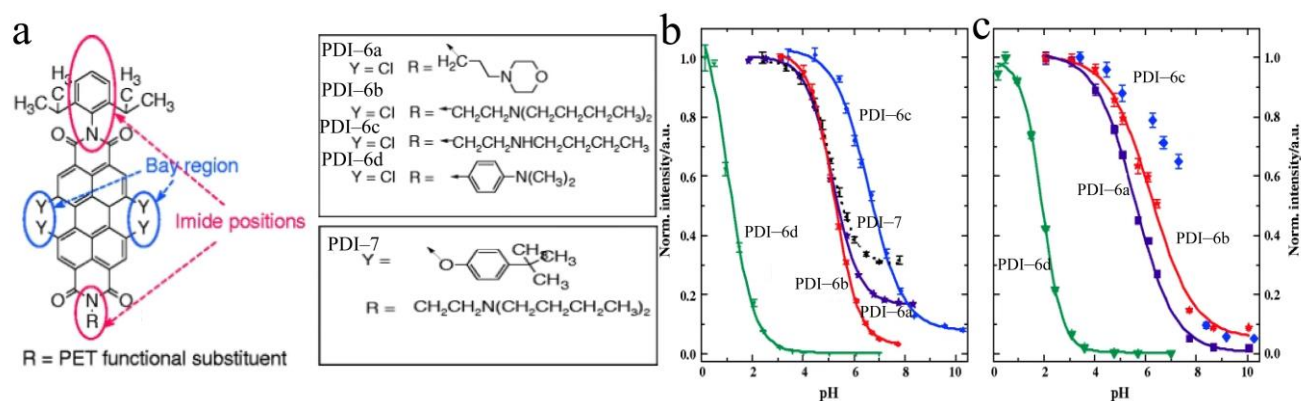
**Figure 4.** (a) Structures and molecule orbital diagrams of single-molecule probe PDI-3 in the unbound and bound states; (b) Absorption and fluorescence spectra of free base PDI-3 in dioxane  $2 \times 10^{-6}$  M (dotted) and the protonated state formed after addition of  $6.5 \times 10^{-3}$  M of HCl (solid); (Inset) Fluorescence titration curve obtained by increasing the concentration of HCl. Reproduced with permission from Ref. [14].

Figure 5a,b present two pH probes based on PDI backbone with single and double modification of the phenylimidazole group at the bay area [12]. The phenylimidazole substitution endows high  $pK_a$  values, enabling a sensing response at high pH values in alkaline solutions (Figure 5c). Benefiting from the inherent high emission brightness and photostability of PDIs, these probes can be immobilized into non-fluorescent plastic matrix (e.g., polyurethane hydrogel) for portable and visible pH probing (Figure 5d,e). Interestingly, the deprotonated state demonstrates extensive bathochromic shift in both absorption and emission spectra compared to the neutral state, which is mainly due to the strong  $\pi$ -conjugated charge transfer interaction between phenylimidazole and PDI. This unique feature makes the probes capable of ratiometric sensing. This series of sensors can not only be used for  $CO_2$  detection, as evidenced with PDI-2 (Figure 3), but they also have great potential for probing pH under alkaline conditions, such as the surface of concrete or alkaliphilic micro-organisms [12].



**Figure 5.** (a) Absorption and emission spectra of the neutral form (black), monoanionic form (red) and dianionic form (blue) of PDI-5 in THF; (b) Equilibria of the neutral and anionic forms of PDI-4 and PDI-5; (c) Corresponding absorption and fluorescence calibration curves of pH sensing of PDI-4 embedded in polyurethane hydrogel D4; Photos of sensor foils under (d) daylight and (e) UV illumination ( $\lambda = 365 \text{ nm}$ ). Reproduced with permission from Ref. [12].

Similar hydrogel sensors were fabricated with a series of asymmetric PDIs modified by different groups at the imide and bay positions, namely tetrachloro PDI-6a to PDI-6d and tetraaryloxy PDI-7 (Figure 6a) [10]. The substituents, especially aliphatic and aromatic amines, provide tunable balance between molecular solubility, amine functionality ( $pK_a$  value and sequence protonation capability) and fluorescence brightness (with quantum yields exceeding 75% in the protonated form). The PET-based pH sensing responses in association with different molecular architectures are shown in detail in Figure 6b,c, where polyurethane hydrogel D4 and poly(hydroxyalkylmethacrylates) were used as polymer matrices, respectively, for non-covalent physical encapsulation of PDIs. According to the dynamic pH value curves of these probes, it can be concluded that an enlarged sensing response range (over 4 pH units) was achieved. The different substituent groups (i.e., tetrachloro or tetra-*tert*-butyl-aryloxy) at the bay area significantly affect the molecular optical features, for which the latter brings out bathochromically shifted absorption and emission spectra and unmatched photostability (the former suffered from photodegradation) but longer response time (slow dynamic response and signal drift). The slow sensing response may be further improved by structure optimization and covalent immobilization into hydrogel network. Nevertheless, all probes showed virtually negligible cross-sensitivity to ionic strength.



**Figure 6.** (a) Molecular structures of PDI-6a to PDI-6d and PDI-7; Calibration fluorescence curves for the pH probes in (b) polyurethane hydrogel D4 and (c) poly(hydroxypropylmethacrylate). Reproduced with permission from Ref. [10].

Considering the importance of a strong acid environment in living species and some physiological processes, appreciable fluorescent probes that can detect lower pH (<4.0) in extremely acidic media were also reported [13,15], as shown in Figure 7a–c. The sensor reported was PDI-8, which bears side group substitution at both imide positions. The side group is composed of an imine (-C=N-) terminated with a thiophene and connected to PDI via two carbons. Due to the lowered  $pK_a$  of the imine unit ( $pK_a = 3.0$ ), PET sensing was found in much more acidic pH value ranges of 2.6–4.0 in DMF/HEPES (*v/v*, 4/1) solutions [15]. Similar probing of low pH in the range of 3.10–4.32 was also reported for PDI-9 (Figure 7d,e) in EtOH/Citric acid-disodium hydrogen phosphate buffer (*v/v*, 1:1) solution, for which the side group substitution was also imine ( $pK_a = 3.69$ ) but terminated with furan [13]. These PET-based fluorescence “off-on” responses were reversible upon a protonation and deprotonation cycle and exhibited great resistance to interference from other common cations and anions. Due to the high emission quantum yields and large Stokes shift, the pH response can even be seen with naked eye, as revealed by the drastic color changes under UV light and daylight, implying the capability of dual-mode sensing. Thanks to their good solubility, PDI sensors can feasibly be employed in portable solid-state pH probing upon blending the fluorophores with test paper or cotton.

Unlike the above-mentioned molecular architectures, recently, there has been an increasing use of dendrimers (containing three-dimensional branching structures) modified with PDI core in organic electronics, bioimaging, sensors and gene delivery, etc. [28,29]. The substitution of PDI at the imide position with light-harvesting electron-donating dendrimers can not only increase the molecular solubility but also endow a strong PET effect within the macromolecule systems, thus enabling fluorescence sensing of proton (pH probing) and metal cations [20,26]. Among them, dendritic polyamidoamine (PAMAM) has attracted considerable attention, which can enable PDI-10 (Figure 8a) with the presence of the tertiary amine receptor unit and long alkylamine terminal groups, having good organic solvent solubility and fluorescence “off-on” pH sensing activity ( $pK_a$  values of 1.8 and 4.1) [26]. In contrast, tetraester PDI-11 (Figure 8a), with  $pK_a$  value of 3.4, showed very distinct fluorescence emission enhancement after acidification of the DMF solution (Figure 8b) [26]. In alkaline media, both molecules will aggregate, leading to quite weak fluorescence. As demonstrated in Figure 8c, PDI-11 has a relatively strong fluorescence intensity under acidic pH range, perhaps due to the conformational difference arising from the larger branch side-chain dimension of PAMAM than tetraester.

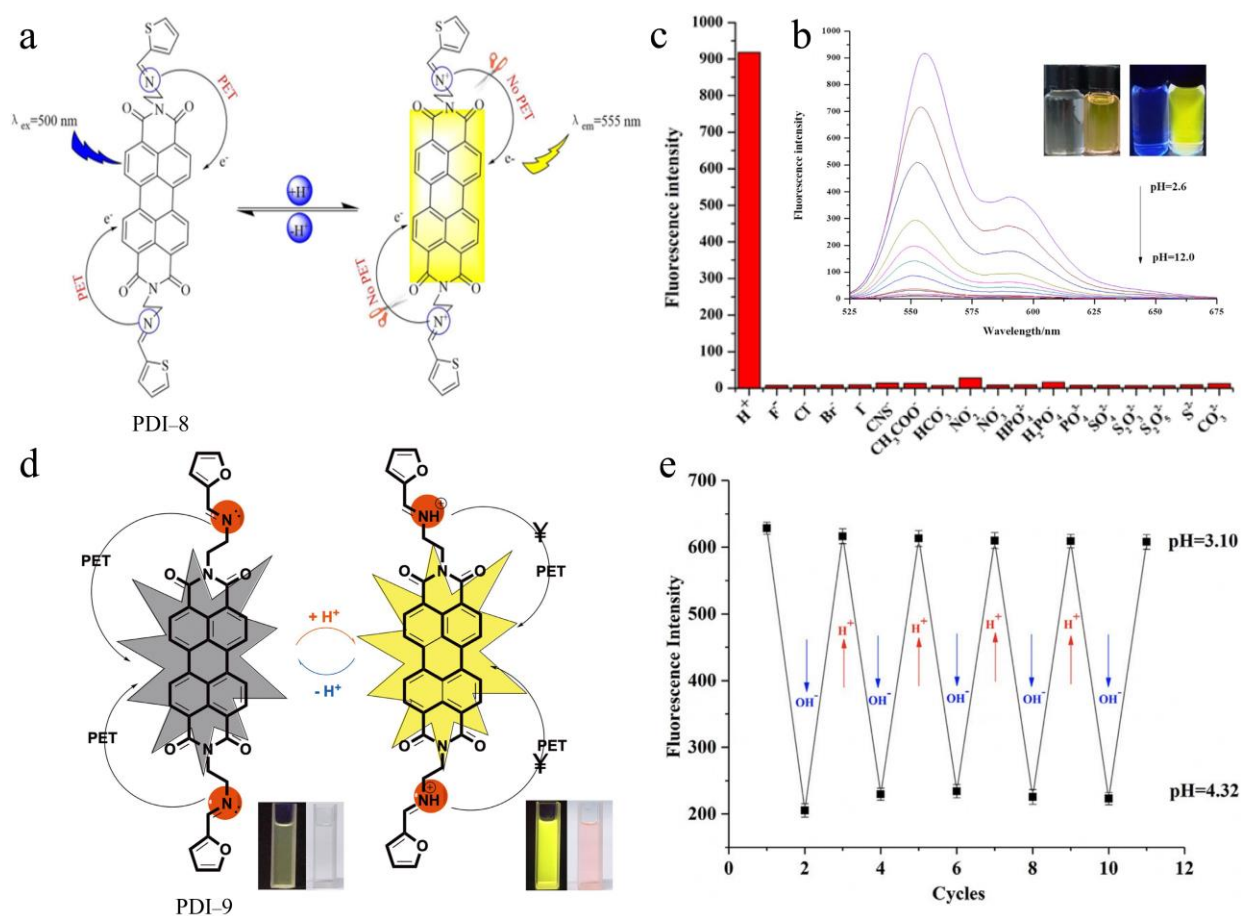


**Figure 7.** (a) Scheme of PET-based pH sensing mechanism of PDI-8 probe; (b) pH-sensitive fluorescence spectra of PDI-8 (10  $\mu$ M) in DMF/HEPES (*v/v*, 4/1) buffer solution and the corresponding photographs taken under daylight (left) and UV light (right), respectively; (c) Selectivity test of the fluorescence response of PDI-8 toward  $H^+$  compared to other anions (50  $\mu$ M, pH = 2.6) in DMF/HEPES (*v/v*, 4/1) buffered aqueous solution. Reproduced with permission from Ref. [15]. (d) Scheme of PET-based pH sensing mechanism of PDI-9 and pH-sensitive color change under UV light (left) and daylight (right), respectively; (e) Reversibility of the fluorescence intensity modulation tested for PDI-9 between pH 4.32 and 3.10. Reproduced with permission from Ref. [13].

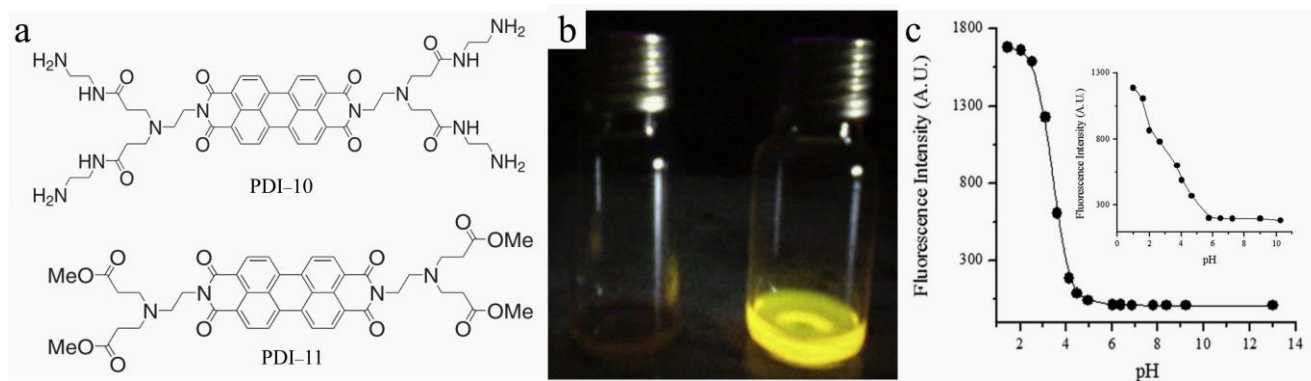


**Figure 8.** (a) Molecular structures of PDI-10 and PDI-11; (b) Photos of PDI-11 in DMF (left) and in DMF after addition of hydrochloric acid (right); (c) Fluorescence intensity curves ( $\lambda_{ex} = 545$  nm) of PDI-11 and PDI-10 (inset) in water/DMF (1:1, *v/v*) as a function of pH. Reproduced with permission from Ref. [26].

### 3.2. pH Sensing Based on Supramolecular (De)Aggregation Mechanism

Supramolecules, as one type of the most investigated biomimetic architectures, have been widely used in chemosensors. On account of the planar molecular skeleton of PDI, PDI molecules have a high tendency to stack, forming supramolecular assemblies via weak interactions, such as  $\pi$ - $\pi$  interaction, and hydrogen bonding, etc. [1]. Thus, PDIs have been recognized as one of the extensively studied artificial building blocks in supramolecular chemistry, including chemosensing [2,30]. Given the fact that pH control is usually critical for the optimized aggregation behavior and shape-defined assembly morphology of PDIs molecules, as well as their uses for ion sensing in the liquid phase [3,31,32], PDI-based fluorescent sensors have demonstrated great potential for use in pH probing or detection of pH-related ions [3,16,17].

Unlike the PET-based fluorescence response upon protonation with  $H^+$ , the fluorescence and other photophysical properties of PDI supramolecules can be modulated by the stimulation of  $H^+/OH^-$  variation in external aqueous environment, which may cause dramatic structural and morphological changes to the supramolecular assembly. For example, pH stimulus can drive the reversible conversion from quenched assemblies to the fluorescent molecule of PDI-12 (Figure 9) [16]. Such (de)aggregation induced pH response takes advantage from its considerable water solubility due to the two ionized amino-imidazole groups grafted on the  $\pi$ -conjugated PDI core. The amino group acts as a protonation site, showing response to pH simulation. PDI-12 was successfully used in detecting pH change due to the formation of gluconic acid from the reaction between glucose and glucose oxide. This implies the potential of using PDI-12 in monitoring in situ the presence of glucose, as well as other bio-species in biofluids or intracellular microenvironments. In another example [17], the solubility of PDI-13/14/15/16 was adjusted by bay substitution, while the imide positions were grafted with different protonated tertiary amine groups possessing variable electron-donating characteristics and alkylcarbonyl linkers with different lengths (Figure 10). Such series of PDI-based pH probes were investigated in HCl/THF solutions with different concentrations. In addition to  $\pi$ - $\pi$  stacking, hydrogen bonding and hydrophobic interactions, the controlled charge interactions between large rigid  $\pi$ -core and the PDI core in relation to the tuned protonation degree have a significant influence on the pH induced self-assembly morphology of PDI molecules. Upon protonation, a large Stokes shift of the emission spectra occurred, accompanied by a fluorescence color change from red to blue of PDI-13, PDI-14 and PDI-15.

### 3.3. pH Sensing Based on Fluorescence Resonance Energy Transfer (FRET) Mechanism

In addition to the above-mentioned shape-defined supramolecular assemblies (e.g., nanofibers), some other supramolecular architectures can also be utilized in pH sensing. Inspired by the natural amphiphiles forming biological bilayer membranes in living vesicle systems, some amphiphilic building blocks of PDIs have been synthesized and used for chemosensors [18,33]. By functionalizing the hydrophobic skeleton of PDI with asymmetric hydrophilic and hydrophobic groups at its imide positions, amphiphilic derivatives PDI-17 and PDI-18 (Figure 11) and the sensing performance were reported [18]. Such water-soluble molecules can be co-assembled into a bilayer nanoscopic vesicle (acting as an energy acceptor) in aqueous solution, for which water-soluble energy donors can be enclosed inside the vesicle. By adjusting the spectral overlap of donors and acceptors, a controlled pH-sensitive FRET process from the "core" (encapsulated donor) to the "shell" (bilayer dye membrane) can be realized, so as to drive the optical sensing application of such nanocapsule vesicle in aqueous solutions. Ultrasensitive pH response was obtained for the nanocapsule sensor as tested in a wide range of pH 3.0–11.0; the sensing response was revealed as dramatic fluorescence color change, covering the whole visible light range under UV (366 nm) illumination.

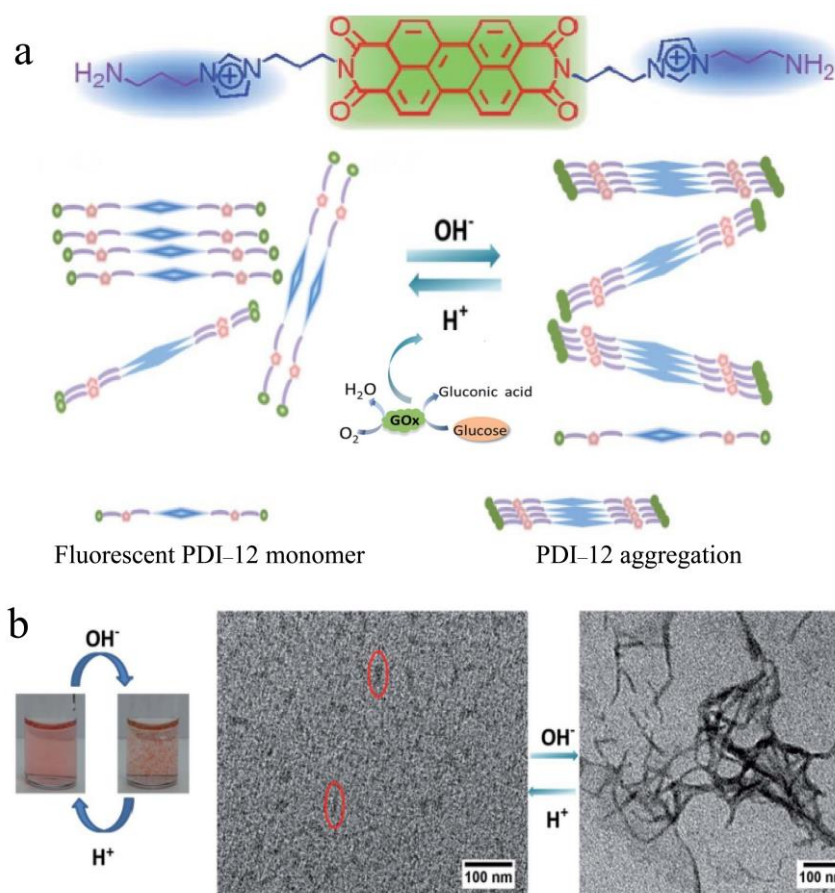


**Figure 9.** (a) Molecular structure of PDI-12 and the schematic illustration of pH-sensitive reversible self-assembly and its use in fluorescence glucose detection; (b) Photographs of aqueous solution (0.5 mM) of PDI-12 at pH 4.0 (left) and pH 8.0 (right) and the TEM images of PDI-12 at pH 4.0 (left) and pH 7.0 (right). Reproduced with permission from Ref. [16].

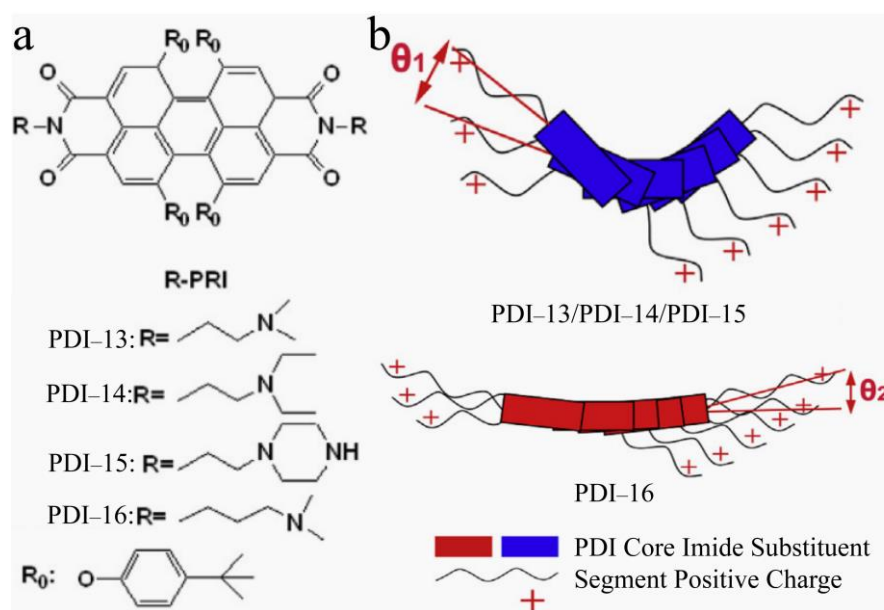


**Figure 10.** (a) Molecular structures of PDI-13/14/15/16 and (b) proposed self-assembly scheme for the nanofibers formed upon protonation. Reproduced with permission from Ref. [17].

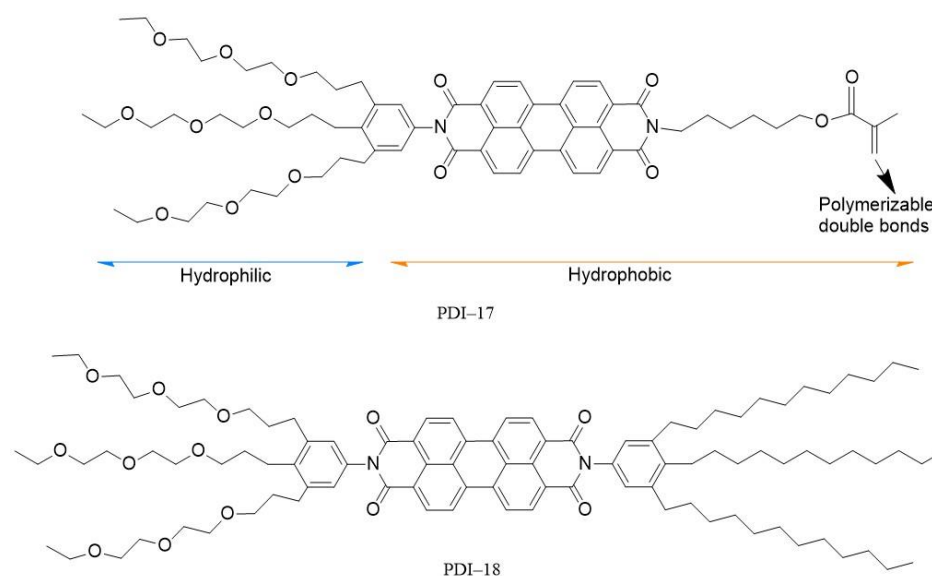


**Figure 11.** Molecular structures of PDI-17 and PDI-18.

### 3.4. pH Sensing Based on Tunable Lateral Dimensions of 1D Nanostructures

Unlike the pH-triggered aggregation–deaggregation process, an alternative way to realize the pH sensing response in water using PDIs is through tuning the lateral morphology of 1D assembly, as evidenced with a histidine-modified PDI-19 molecule (Figure 12) [19]. With histidine auxiliaries, PDI-19 demonstrates bio-inspired bolaamphiphility in the zwitterionic form under physiological pH, which plays with the two  $pK_a$  values of 4.1 (carboxylic acid) and 7.3 (imidazole ring). The 1D self-assembly of PDIs is highly dependent on the molecular structure of substituents at the imide position in association with the various non-covalent intermolecular interactions (e.g., electrostatic attraction/repulsion, hydrogen bonding, etc.), which in turn can be initiated and tuned by pH change through the protonation–deprotonation process. It was found that the lateral dimension of the assembly of PDI-19 was reversibly transformed from thick fiber (at pH = 7) to thin fiber (pH = 10) and belt (pH = 2), and this resulted in a corresponding change in fluorescence accompanied by supramolecular chiroptical switching (left-handed to right-handed helical self-assembly). Taking advantage of the reversibility of the pH induced structural and property change, the reported PDI system may help develop new application scenarios for pH probing in water, capitalizing on the unique features of chiroptics and biomedicine.

### 3.5. pH Sensing Based on Volume Phase Transition of Unimolecular Micelle

Compared to the dimensional change of 1D molecular assembly, structure-controllable unimolecular micelles can also be developed into optical chemosensors reliant on the pH induced structure change. Upon substitution with sufficiently large dendrimers, PDI-20 and PDI-21, as shown in Figure 13a, can behave as a unimolecular micelle with the core being hydrophobic and the shell hydrophilic. The globular “core–shell” morphology (average diameters around 20 nm) makes the micelles a unique platform to be used in pH probing in complete aqueous media (pH = 7) (Figure 13b) [20]. These micelles displayed reversible volume phase transition around their  $pK_a$  values (6.34 and 8.05, respectively) due to the ionization (fully charged state; size increasing) or deionization (totally uncharged state; size decreasing) of the polymer chains induced by pH variation (Figure 13b). Accompanying size change, the significant change of fluorescence can be used as sensor signals for probing the pH (Figure 13c). It is the flexible cationic or anionic polyelectrolyte side chains as the outer shell, which contributes to high water solubility (>10 g/L) and high fluorescence quantum yields in water (0.11 for PDI-20 and 0.13 for PDI-21) by preventing the central PDI chromophore from aggregation, for which the electrostatic repulsion capability (in relation to the polymer chain stretching or collapsing) is highly dependent on pH.

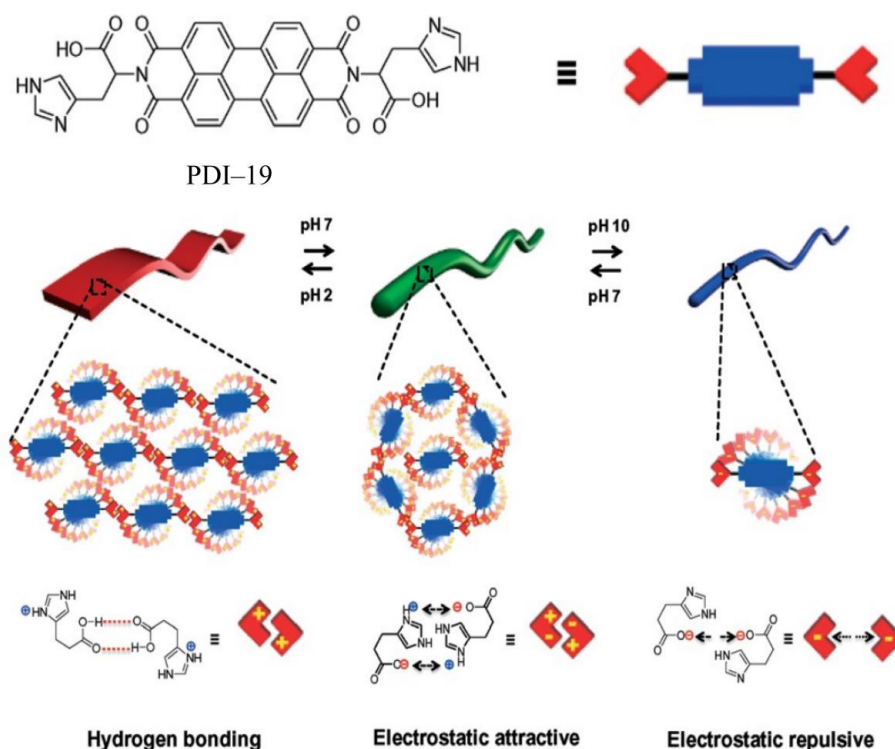


**Figure 12.** Molecular structure of PDI-19 and schematic illustration of the reversible morphology and chiral self-assembly switching in water induced by pH change. Reproduced with permission from Ref. [19].

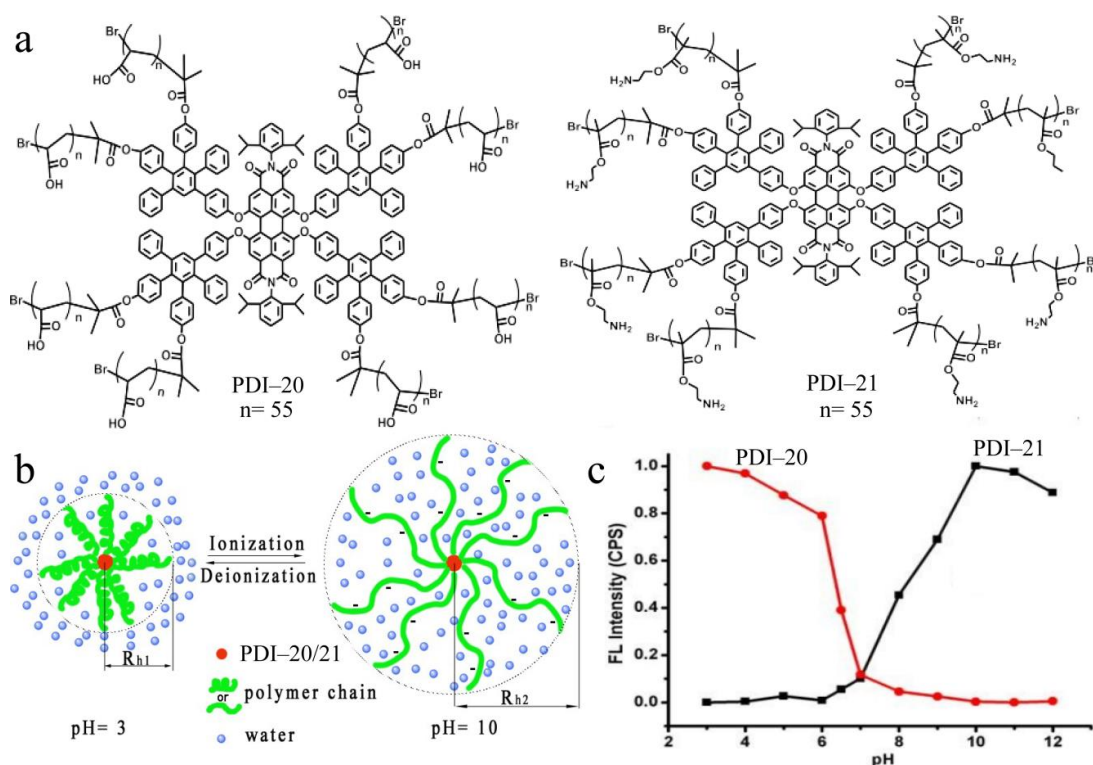


**Figure 13.** (a) Molecular structures of PDI-20 and PDI-21; (b) Schematic volume phase transition of PDI-20/21 unimolecular micelle; (c) Normalized peak fluorescence intensities (at ~620 nm for PDI-20 and ~607 nm for PDI-21) as a function of pH as tested in Tris-HCl buffer. Reproduced with permission from Ref. [20].

### 3.6. pH Imaging in Cells

External pH stimuli or an acid-base microenvironment are extremely crucial for cell survival as well as its internal and external physiological/pathological activities *in vivo*, and therefore, accurate *in situ* probing of the pH would help in health monitoring and disease diagnosis [9,24,34]. PDIs as fluorophores for pH monitoring in cells have gained particular interest mainly because of the advantages in the following aspects [13,21–24]: versatile molecular design, robust structure with combined chemical/photochemical/thermal stability, lower biological toxicity, high fluorescent emission brightness (intensity) under lower excitation energy, lower auto-emission and light scattering interference from intracellular microenvironments, desired cell penetration capability, etc. Further support comes from the essential light penetration across tissues and multidimensional analysis ability of the fluorescence technique itself. The key challenge remaining for PDI-based sensors lies in their hydrophobic skeletons and aggregation-induced weak emission intensity in aqueous solution. To date, amphiphilic PDIs with good solubility and biodistribution in water are the most preferable architectures for intracellular pH probing via fluorescence intensity or lifetime modulation as the signal.

#### 3.6.1. Dendritic PDIs for Live-Cell Imaging

The water-soluble PDI–20 and PDI–21 shown in Figure 13 [20] possess macromolecular scale architecture, which may only be acceptable for environmental and extracellular biofluid probing. Relying on the large branched oligo (glutamic acid) group with PEG chains, a water-soluble dendritic molecule PDI–22 (Figure 14a) was synthesized as a fluorescence probe for live-cell imaging [21]. Although the PEG chains bring less cytotoxicity in aqueous solution, the molecule size otherwise seems too bulky for cell penetration. Nevertheless, in view of the presence of protonatable groups in the side chains, this molecule may be a good candidate for extracellular pH probing.

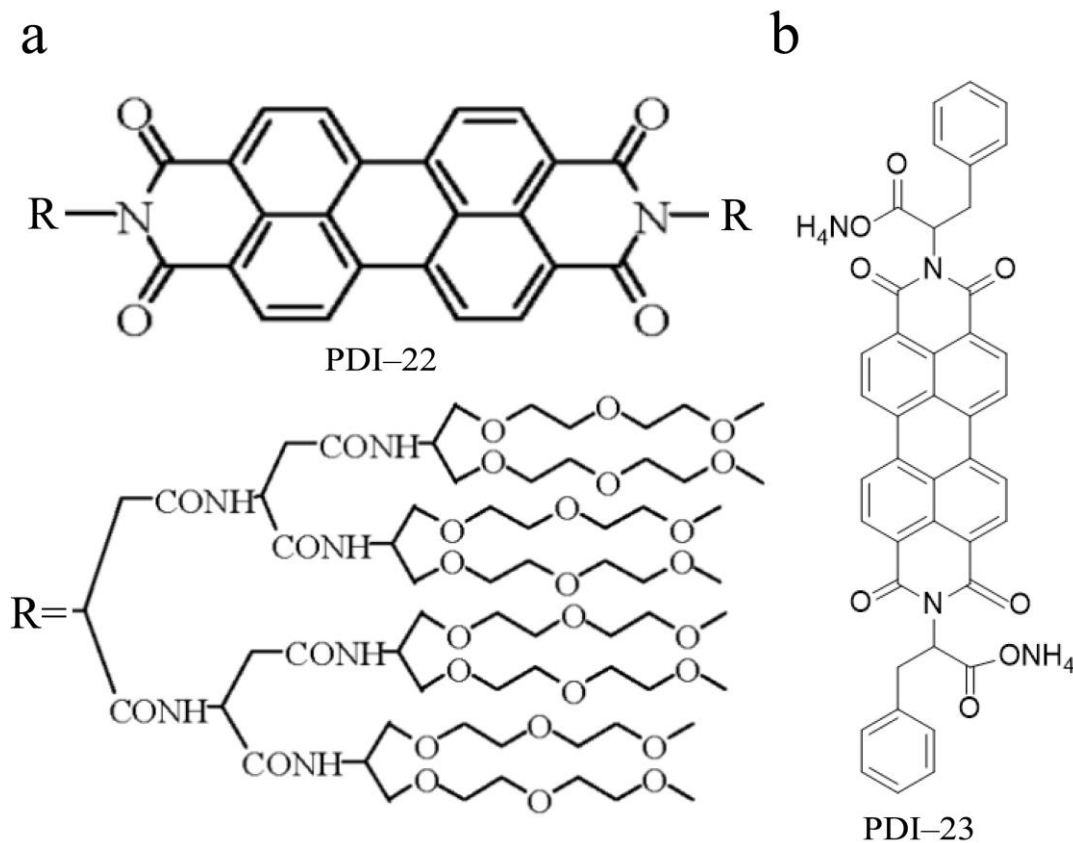


**Figure 14.** Molecular structures of (a) PDI–22 and (b) PDI–23.

In comparison, a much simpler amphiphilic PDI–23 modified with amino acid as side groups (Figure 14b) has been synthesized and studied for fluorescence probing of pH in water and living cells [22]. It is the intermolecular electrostatic repulsion between hydrophilic phenylalanine amine side chains, which enables its good water solubility and low cytotoxicity. PDI–23 showed a pH-dependent fluorescence response over a wide range of pH 4.0–7.0, which was suitable for extracellular and intracellular pH probing in living HeLa cells controlled by phosphate-buffered saline (PBS) buffer. Under UV light irradiation ( $\lambda = 330\text{--}380\text{ nm}$ ), a weakened fluorescence brightness occurred in accordance with the pH change from 7.0 to 5.5 and 4.0. Promisingly, a ratiometric response with two excitation or emission wavelengths was demonstrated for such pH-sensitive probe, which had concentration-independent reliability and accuracy.

In view of the important role of neutral and weakly acidic pH determination in abnormal physiological process detection, another PDI probe PDI–24 (Figure 15a), with  $pK_a$  of  $6.35 \pm 0.02$ , was synthesized and studied for intracellular pH probing of L929 cells [23]. To be more precise, its “water-soluble” fluorescence feature was actually based on the nano-sized aggregates (with hydrodynamic diameter of 122.4 nm), which can be well dispersed in water. The non-toxicity of this probe was proven, as tested in a broad concentration range from 330  $\mu\text{M}$  to 1.3  $\mu\text{M}$  of L929 cells (Figure 15b). However, pH-sensitive fluorescence emission was only observed at 1.3  $\mu\text{M}$  concentration, whereas this was not applicable to a much higher concentration above 26  $\mu\text{M}$  owing to substantially increased aggregation.

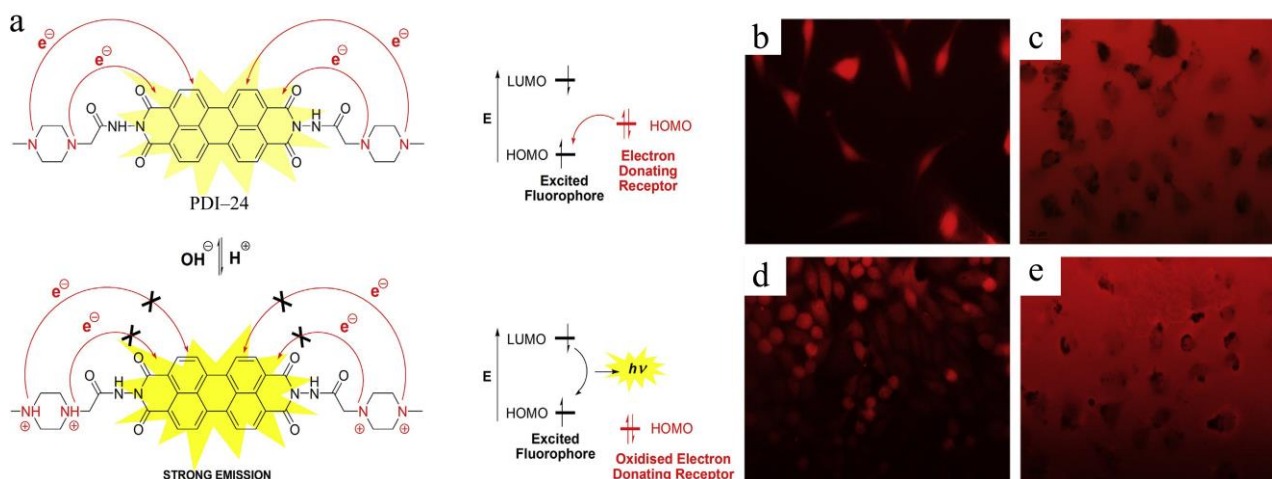


**Figure 15.** (a) Molecular structure of PDI–24 and its photophysical mechanism for pH probing; (b–e) Fluorescent photographs (under bars of 50  $\mu\text{m}$ ) of PDI–24 micelles in living L929 cells. The cells were incubated for 24 h (upper) and 48 h (lower) with PDI–24 concentrations of 1.3  $\mu\text{M}$  (b,d) and 26  $\mu\text{M}$  (c,e). Reproduced with permission from Ref. [23].

### 3.6.2. Fluorescence Lifetime Probing

Along with the inhibited PET process (fluorescence “turn-on”), the protonation of amine groups (the free base form of the PDI molecule) could also cause a decrease in fluorescence lifetime, which can be used as another sensing signal for pH imaging in cells [24]. Although there is less related research compared to that performed on fluorescence intensity, such sensing mode becomes quite promising for biological imaging due to its independence from fluorophore concentration, fluorescence intensity, excitation wavelength and duration of light exposure [25].

By comparing PDI–25 linked to cell-penetrating moieties with PDI–26 immobilized in cationic hydrogel nanoparticles (Figure 16a), it was found that, although the former, as a molecular probe, presented rapid cell penetration and bright staining, only the polymeric nanoparticles were capable of quantitative fluorescence lifetime response to intracellular pH. In live cells, PDI–26-based nanoparticle probe showed stable pH calibration and high-resolution lifetime changes from 4.7 to 3.7 ns between pH 4.4 and 8 (Figure 16b,c). It may be

that the unstable calibration and microenvironment disturbance of lifetime signal, as well as molecular aggregation tendency, resulted in fluorescence quenching, which limited the use of the molecular probe in this aspect [24]. PDI-27, a simple structure with symmetric substitution by N-hydroxyethyl-aminoethyl groups at the imide positions (Figure 17), was also found to be capable of pH probing via measurement of the fluorescence lifetime response in living C3H10T1/2 cells [25]. The protonation of secondary amine groups in the side chains not only inhibits the intramolecular PET of PDI-27 (thus turning on fluorescence) but also molecular aggregation owing to the intermolecular electrostatic repulsion between the protonated (cationic) chains in acidic solution. Conversely, deprotonation under basic pH facilitates molecular aggregation, resulting in fluorescence quenching. Since the protonated state was quite stable, the fluorescence lifetime could be reliably measured, and the lifetimes obtained showed a linear response toward pH value changing in the range of 6–8 ( $pK_a = 7.4$ ) within  $\sim 2$  ns change, as tested in Tris·HCl buffered solutions, synthetic intracellular buffer (SIB) or C3H10T1/2 mesenchymal cells. The maximum fluorescence lifetime of SIB solution ( $\sim 2.5$  ns) was shorter than that of Tris·HCl buffered solution ( $\sim 4.2$  ns) under pH < 6.0 condition due to the influence of salts and macromolecules present in SIB. One shortcoming is that such PDIs without bay modification and large-volume imide substituent cannot be well dispersed in the cytosol.

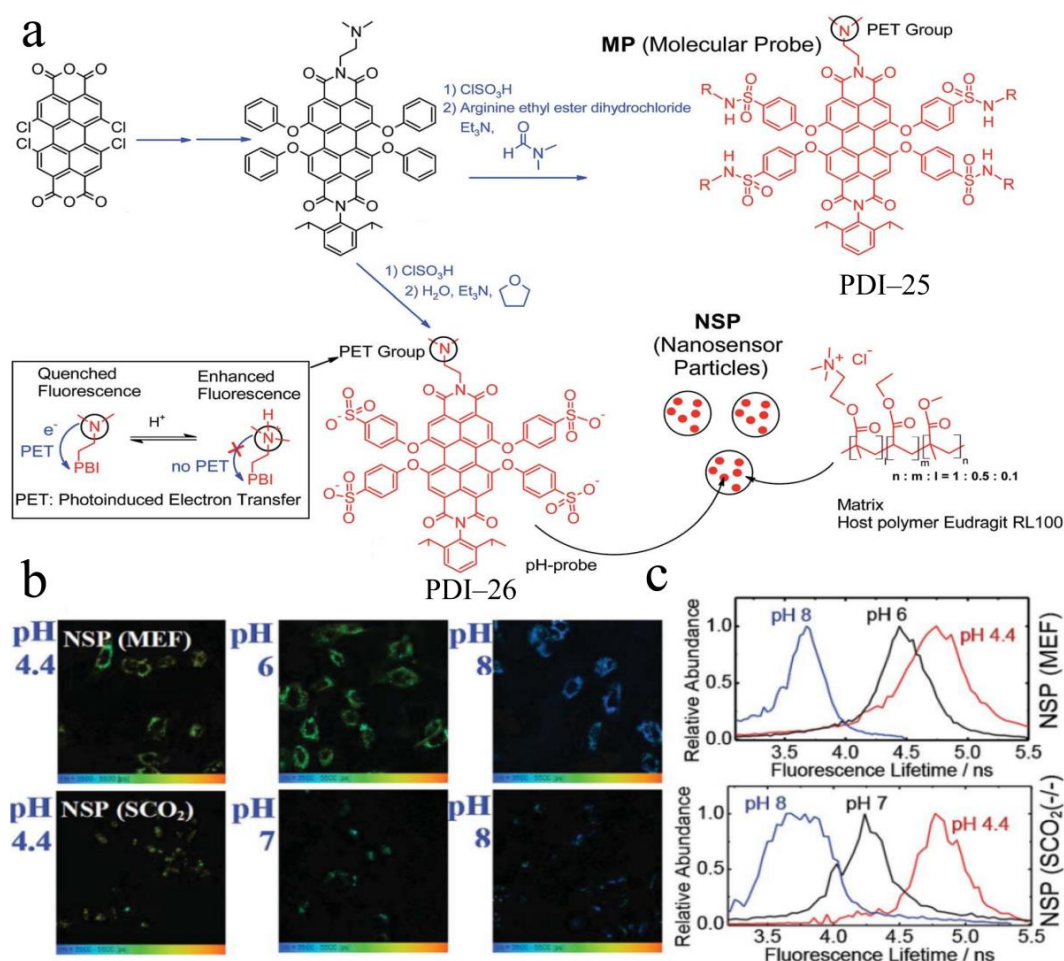


**Figure 16.** (a) Molecular structures of PDI-25 linked to cell-penetrating moieties and PDI-26 immobilized in cationic hydrogel nanoparticles and their photophysical mechanism for pH probing; (b) False-color images of PDI-26-based pH response of mouse embryonic fibroblast (MEF) or human colon cancer cells HCT116 ( $SCO_2$ ); (c) Their corresponding distributions of fluorescence lifetimes in the images. Reproduced with permission from Ref. [24].

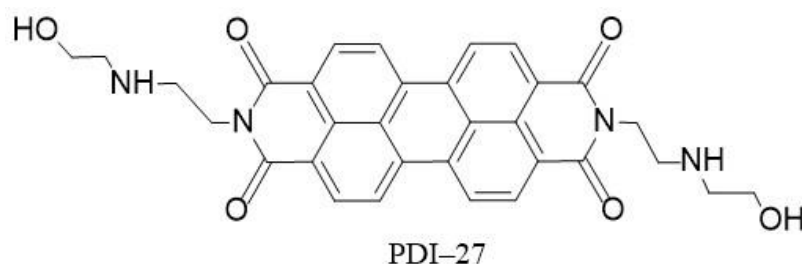


Figure 17. Molecular structure of PDI-27.

#### 4. Conclusions and Perspectives

The precise control and probing of the pH remain critical for the monitoring of health, biological, industrial and environmental analysis processes, as well as the detection of other ionic species, such as metal ions, for which the sensitive or selective measurement by chemical sensors is often dependent on the pH of the sample. As described in this review, the change in pH can be monitored through colorimetric and fluorescent sensors (via modulation of the emission intensity or lifetime). PDIs, as a series of extensively studied optical chemosensors, exhibit comprehensive advantages, including unique photophysical properties together with high photostability, abundant structure adjustment and facile synthesis, intrinsically supramolecular aggregation/deaggregation and highly controllable PET through protonation/deprotonation of the electron-donating groups. This review is expected to provide an insight into the design of new PDI structures and beyond, so as to further improve the pH probing performance regarding both sensitivity and selectivity, as well as the expanded application in aqueous media, including live cells.

Despite great progress having been made, there are still some critical challenges for PDI-based pH sensing, which should be addressed with more research. For example, in comparison to the environmental and industrial analysis, pH probing in real time would be more favorable for living physiological processes and biomedical systems [9,15]. However, relatively fewer molecular architectures of PDIs have been investigated, and moreover, the quantitative or ratiometric measurements of pH with PDI-based sensors are usually more difficult than those used for measurement of other ionic analytes [3]. In addition, the influence of temperature on pH sensing of PDIs and the associated molecular aggregation (in line with solubility, photophysical properties, etc.) should be taken into account in future research, particularly regarding the molecular structure design of sensors. Additionally, in contrast to the fluorescence mode, the colorimetric mode of PDI-based pH sensing has been much less explored to date, while the latter can be more feasibly developed as a device with simpler operation without the involvement and alignment of the excitation light source [3,12,35]. Briefly, some current or recent efforts aiming at addressing the technical changes in PDI-based pH sensors and improving the sensor performance are discussed below.

##### 4.1. pH-Resistant Fluorescence Probes

To broaden the applicability of a single optical chemosensor for rapid ion detection under different pHs without complex sample preparation or processing, it is particularly imperative to develop pH-resistant fluorescence probes. This could be one of the promising research directions for future endeavor. Indeed, most of the fluorescence probes developed from organic dyes, including PDIs, are only functional for the quantitative analysis of protons or other ions within a narrow dynamic range of pH [9,10]. This seriously limits the practical application scope, as the real sample or environment may keep changing in terms of the pH, which otherwise requires constant monitoring and control of pH in the measurement process, thus making the test process complicated and time consuming.

A cationic PDI probe, PDI-28 (Figure 18), was reported, which was water-soluble and remained fluorescent in water. This probe demonstrated selective fluorescence “on-off” response toward 4-nitroaniline (4-NA) and picric acid (PA) without significant interference

from other nitroaromatic compounds, as tested in DMF/water or aqueous medium across a wide pH range (1 to 10) [36]. In comparison, the other two analogs, PDI-29 and PDI-30, as well as the non-ionic version (PDI-31), can also realize the same but weaker response. These observations suggest that with appropriate side group modification, the PDI probe may tolerate more pH change while still maintaining the fluorescence sensing response.

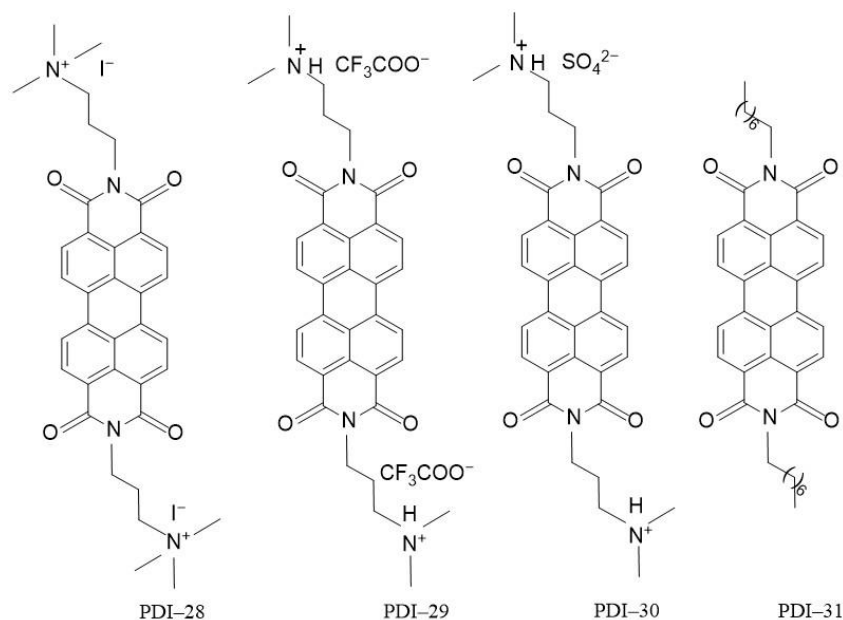


**Figure 18.** Molecular structures of PDI-28 to PDI-31.

#### 4.2. pH Response within Strong Acidic or Basic System

The detection of pH change in strong acidic or basic environment still remains a challenge [9], as most of the sensor molecules or materials (whether organic or inorganic) become chemically unstable under the extreme condition. Taking advantages of the unique conjugation structure of PDI and substitution tunability at the bay area, some successes have been achieved in PDI-based sensor systems, which are capable of detecting pH change in the region of  $\text{pH} < 1$  and  $\text{pH} > 11$  [30,35].

As shown in Figure 19, by forming a twisted molecular structure via 1,6,7-trisubstitution at the bay area, PDI-32 exhibited dramatic absorption and emission spectral change (Figure 19b,c) in the visible region upon change in pH in the extremely acidic medium ( $\text{pH} 1.0$  to  $-0.6$ ) [20,35]. Accompanying the spectral change was the distinct color change and fluorescence off-on switching, as tested in both the solution phase and on a solid substrate, such as a paper strip (Figure 19d). A combination of the colorimetric and fluorescence sensing mode makes it possible to develop PDI-32 as a dual-mode sensor for detecting high concentrations of strong acids, such as HCl,  $\text{H}_2\text{SO}_4$  and  $\text{HNO}_3$ , whereas the presence of common weak acids, such as acetic acid and carbonic acid, would pose no significant interference. The strong electron-donating characteristic of two piperidinyll moieties and their capability of successive protonation into  $\text{PDI-32H}_2^{2+}$  ( $\text{pK}_a$  ca. 0.82) are believed to be the reasons for the observed spectral changes, for which the double protonated state of  $\text{PDI-32H}_2^{2+}$  becomes inactive in the charge transfer transition (Figure 19a). The multiple resonance structures available for the protonated PDI-32 help stabilize the molecules during testing (Figure 19a).

As illustrated above, most PDI-based pH probes work only in the near neutral and acidic range, and some meet the development requirements for working under high acid situations [13,15,35] or weak base media [18]. On the contrary, the detection of pH in high base environments seems quite rare, although it remains crucial for monitoring steel anticorrosion and waste water treatment. [37]. This is due to the instability of PDI molecules in strong basic environments, that is, the imide cyclic structure could be opened through

hydrolysis under high pH, yielding perylene tetracarboxylic acids (PTAC) [1]. Nonetheless, this offers an opportunity to develop fluorescent pH probes based on PTAC architecture in alkaline solutions at pH > 10. As shown in Figure 20a, two PTAC derivatives, PTAC-1 and PTAC-2, were synthesized, with the four acids converted to electron-deficient carboxylic ester groups and the bay being substituted with electron-donating groups, such as amine or hydroxyl groups, or electron-withdrawing groups, such as oxygen. These two molecules have adjustable and high pK<sub>a</sub> values of 8–12 depending on the modification of side group substitution. Upon change in the pH, PTAC-1 and PTAC-2 behave as pH indicators, exhibiting reversible fluorescence “on–off” response accompanied by distinct color change. Such response showed great anti-interference from other common metal cations or anions and was proven capable of working as solid-state pH test paper for alkaline pH value monitoring (Figure 20b,c). This study provides valuable insights into the design of new structures beyond PDI, which can extend pH probing into a broader range, especially the high basic region.

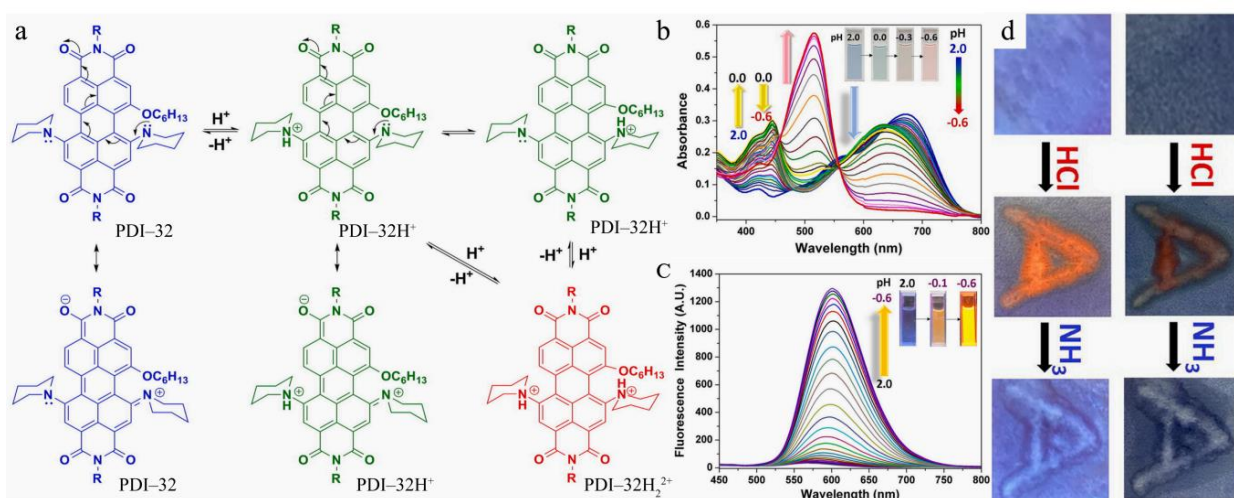


**Figure 19.** (a) Scheme of the possible resonance structure for PDI-32 (PDI-32H<sup>+</sup>), explaining the disappearance of the charge transfer absorption band in PDI-32H<sub>2</sub><sup>2+</sup>; (b) Absorption and (c) fluorescence emission spectra of PDI-32 (5 μM) in the presence of different concentrations of HCl (0.01–4.0 M) in a methanol/water (9:1, v/v) solution; (d) Photographs of test strips of PDI-32 after addition of HCl and NH<sub>3</sub> under ambient (right) and UV light (left). Reproduced with permission from Ref. [35].

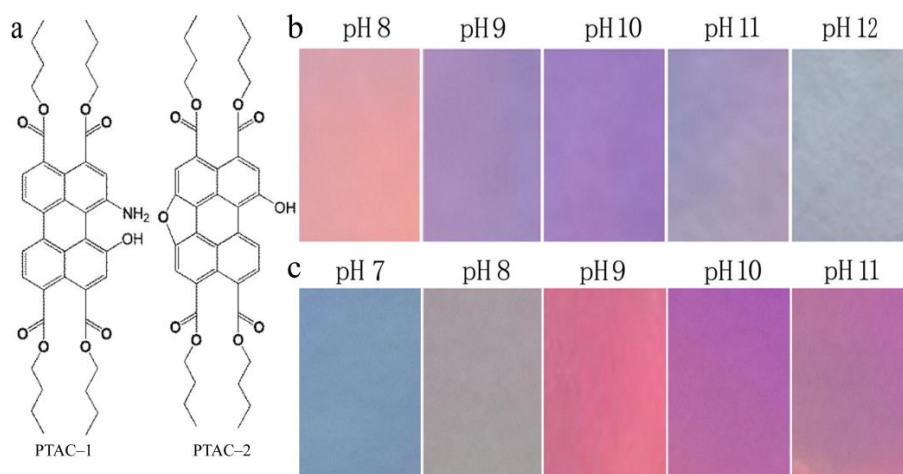


**Figure 20.** (a) Molecular structures of PTAC-1 and PTAC-2; Fluorescence photographs (under 365 nm irradiation) of test strips made of (b) PTAC-1 and (c) PTAC-2 upon exposure to various alkaline pHs. Reproduced with permission from Ref. [37].

#### 4.3. pH Response with PDI-Involved Composites

While some PDIs have been successfully fabricated with other compounds as nanoscopic vesicles and hydrogel nanoparticles and used in pH sensing as mentioned above [18,33], very few other composites (particularly those with inorganic materials) have ever been reported with PDIs as the primary sensor component for detecting pH change. This is likely due to the technical challenge regarding a trade-off between chemical stability and sensing efficiency of PDIs in aqueous media. In general, to maintain the high stability of the composites, the PDI molecules used should have limited solubility in water. However, the limited solubility (often accompanied by low hydrophilicity) would otherwise weaken the sensing interaction with protons. Nonetheless, significant efforts have recently focused on developing inorganic composite sensors or probes by incorporating various PDIs, although these sensors were designed primarily for bioimaging or monitoring of other analytes [38,39]. The common way to fabricate inorganic composite sensors of PDI would be via the functionalization or blending of PDI with organic [40], inorganic [41–43] or organic–inorganic [44–49] counterparts in the form of conjugates or nanoparticles, which are conducive to development of fluorescence bioimaging, NIR-absorbing photosensitizers for photodynamic therapy and environmental or health monitoring [50]. Surface immobilization of PDIs on inorganic nanoparticles, such as silica gels [51,52] and single-walled carbon nanotubes (SWCNTs) [53], has also been reported for fluorescent or colorimetric sensing. Considering that, very often, the optimal sensing responses reported for these composite sensors rely on the control of pH values, the design rules learned therefrom may help adapt some of the composite materials into pH probing, which will certainly require more research effort in structure engineering and optimization.

#### 4.4. pH-Mediated Detection of Other Analytes

In addition to pH monitoring itself, another promising area for PDIs is the development of optical sensors for ions reliant on pH-mediated chemical reactions, for which the small acid or base generated (i.e., the pH change) can be detected in situ by the built-in PDI probe. In general, the small acid or base species that might be generated include HCl, CO<sub>2</sub>, SO<sub>2</sub> and NH<sub>3</sub>. The same probing system may also find application in quantified demonstration of chemical reaction processes in environment or biological systems. Some explorative studies have already been performed in these aspects [12,54,55].

In an example shown in Figure 21a–c, fluorescence “on–off” response toward urea in a urine sample was observed for amphiphilic PDI–33 [54]. The sensing depends on pH-stimulated aggregation–deaggregation of PDIs originating from deprotonation–protonation of their imidazole side groups. The pH change was due to the production of hydroxide ion (OH<sup>−</sup>) from the enzymatic hydrolysis of urea by urease. By detecting precisely the pH change in this case, it becomes feasible to measure the concentration of urea, taking advantage of the high-controlled enzyme reaction. A solid-state gel film embedded with well-dispersed PDI–33 was also fabricated and tested, showing visible fluorescence “turn-on” response toward urea in HCl-methanol media. This type of sensor composite will not only find great potential in development as an instant diagnostic kit for human urine analysis but, more importantly, it will help explore new design rules for PDI molecules, which may be incorporated with enzymes or other catalysts to expand the sensing and detection scope.

Another case of pH-mediated detection, as presented in Figure 21d,e, was recently reported from our lab. PDI–3 was used as a fluorophore to develop a reliable and highly efficient paper-based fluorescence “off–on” sensor for gaseous formaldehyde detection with both low limit of detection (LOD) and extremely high selectivity [55]. The sensing was originated from a specific and quantitative aldimine condensation reaction between formaldehyde and hydroxylamine sulfuric salt ((NH<sub>2</sub>OH)<sub>2</sub>·H<sub>2</sub>SO<sub>4</sub>), and the sulfate acid thus released could be detected by PDI–3 via the PET mechanism, as shown in Figure 4a. Compared with the polymer gel matrices used for supporting the PDI probes as mentioned above, the porous cellulose substrate of paper used in our study not only provides a larger

open surface for the capture and adsorption of gas analytes but is also lower in cost, which can eventually be made disposable as needed.

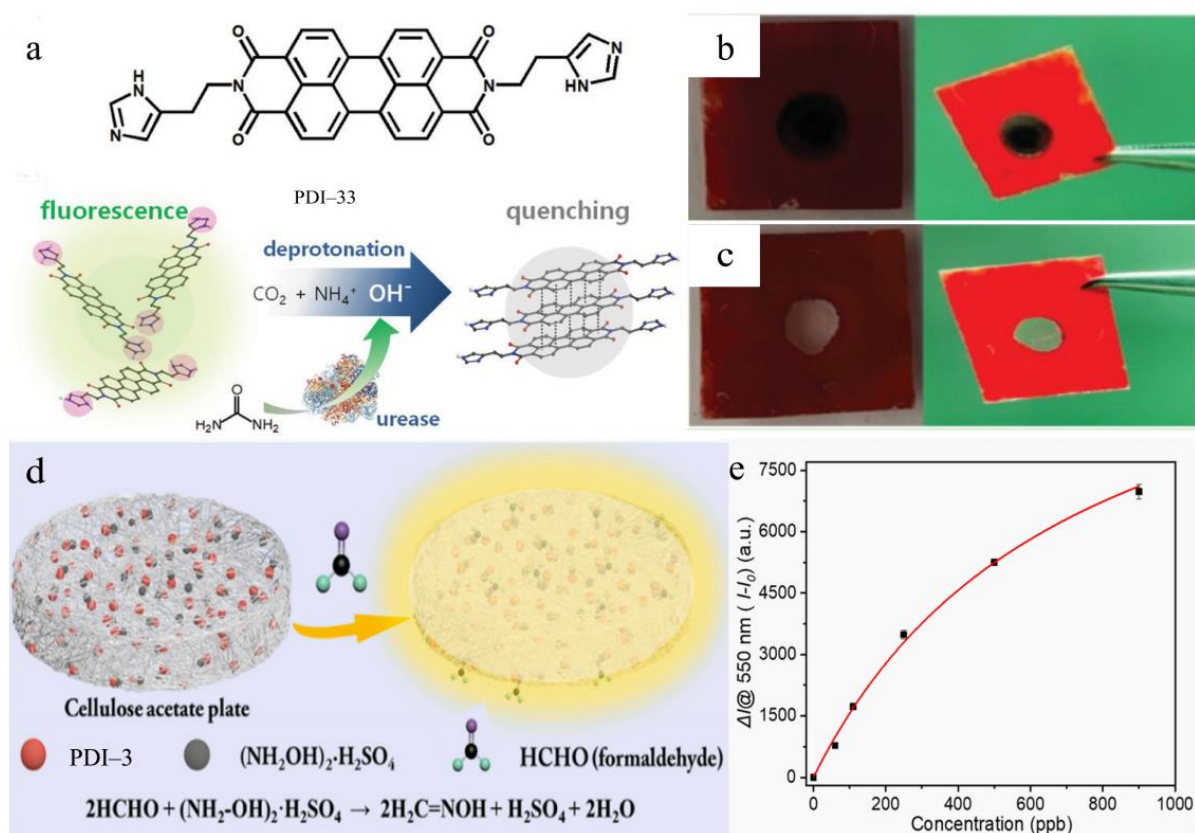


**Figure 21.** (a) Molecular structure of PDI-33 and schematic illustration of its mechanism for urea sensing; Color changes of PDI-33 sensor film after dropping (b) hydrolyzed urea solution over 10 mM and (c) under 10 mM (left: under daylight, right: under green light) (reproduced with permission from Ref. [54]). (d) Schematic illustration of PDI-3-based fluorescence turn-on sensor for gaseous detection of formaldehyde and its chemical reaction mechanism; (e) Increase in fluorescence intensity ( $\Delta I$ ) as a function of the concentration of formaldehyde in gas phase. Reproduced with permission from Ref. [55].

#### 4.5. Integrating pH Probe into Devices

Benefiting from the high versatility of their chemical structures, aggregation state, solubility, etc., PDIs can be entrapped into porous fibrous membranes [20,35,55], sol-gel or hydrogel [10,12,54] matrix to fabricate wearable or stretchable chemosensors for health monitoring or biological sensing in implanted devices. These solid-state fluorescent sensor devices are usually durable, low-cost, portable, tunable in shape and size, possibly recyclable, and so on. With this in mind, improved fabrication techniques for incorporating PDIs into wearable substrates become particularly important and should be further explored in future endeavors [56]. In contrast to the solution-phase pH probing, which is suitable for cell imaging, solid-state wearable sensors are more suitable for non-invasive probing or monitoring, targeting environmental and bio-markers. Furthermore, the integration of a pH sensor with other functional devices (e.g., temperature sensor) would help expand and enhance its application in more diverse scenarios. For example, in combination with a temperature sensor, pH probing could be significantly improved in terms of accuracy by including the temperature effect, which is proven as an important factor in chemical binding and adsorption interaction, which in turn affects the fluorescent sensing response.

**Author Contributions:** Conceptualization, S.C.; investigation, S.C.; writing—original draft preparation, S.C.; formal analysis, resources and software, M.Z. and L.Z. (Ling Zhu); writing—revision and editing, S.C., L.Z. (Ling Zang) and X.Y.; supervision, S.C. and L.Z. (Ling Zang); funding acquisition, S.C. All authors have read and agreed to the published version of the manuscript.

**Funding:** This research was funded by Academic Development Project of TongXin Funds (grant number 2023161802).

**Institutional Review Board Statement:** Not applicable.

**Informed Consent Statement:** Not applicable.

**Data Availability Statement:** Not applicable.

**Conflicts of Interest:** The authors declare no conflict of interest.

## References

1. Chen, S.; Slattum, P.; Wang, C.Y.; Zang, L. Self-assembly of perylene imide molecules into 1D nanostructures: Methods, morphologies, and applications. *Chem. Rev.* **2015**, *115*, 11967–11998. [[CrossRef](#)]
2. Wang, Q.; Li, Z.; Tao, D.D.; Zhang, Q.; Zhang, P.; Guo, D.P.; Jiang, Y.B. Supramolecular aggregates as sensory ensembles. *Chem. Commun.* **2016**, *52*, 12929–12939. [[CrossRef](#)]
3. Chen, S.; Xue, Z.X.; Gao, N.; Yang, X.M.; Zang, L. Perylene diimide-based fluorescent and colorimetric sensors for environmental detection. *Sensors* **2020**, *20*, 917. [[CrossRef](#)] [[PubMed](#)]
4. Ali, S.; Gupta, A.; Shafiei, M.; Langford, S.J. Recent advances in perylene diimide-based active materials in electrical mode gas sensing. *Chemosensors* **2021**, *9*, 30. [[CrossRef](#)]
5. Singh, P.; Sharma, P.; Kaur, N.; Mittal, L.S.; Kumar, K. Perylene diimides: Will they flourish as reaction-based probes? *Anal. Methods* **2020**, *12*, 3560–3574. [[CrossRef](#)]
6. Zhang, M.; Shi, J.F.; Liao, C.L.; Tian, Q.Y.; Wang, C.Y.; Chen, S.; Zang, L. Perylene imide-based optical chemosensors for vapor detection. *Chemosensors* **2021**, *9*, 1. [[CrossRef](#)]
7. Zhou, W.W.; Liu, G.; Yang, B.; Ji, Q.Y.; Xiang, W.M.; He, H.; Xu, Z.; Qi, C.D.; Li, S.; Yang, S.G.; et al. Review on application of perylene diimide (PDI)-based materials in environment: Pollutant detection and degradation. *Sci. Total Environ.* **2021**, *780*, 146483. [[CrossRef](#)]
8. Singh, P.; Hirsch, A.; Kumar, S. Perylene diimide-based chemosensors emerging in recent years: From design to sensing. *TrAC Trends Anal. Chem.* **2021**, *138*, 116237. [[CrossRef](#)]
9. Steinegger, A.; Wolfbeis, O.S.; Borisov, S.M. Optical sensing and imaging of pH values: Spectroscopies, materials, and applications. *Chem. Rev.* **2020**, *120*, 12357–12489. [[CrossRef](#)]
10. Aigner, D.; Borisov, S.M.; Klimant, I. New fluorescent perylene bisimide indicators—A platform for broadband pH optodes. *Anal. Bioanal. Chem.* **2011**, *400*, 2475–2485. [[CrossRef](#)] [[PubMed](#)]
11. Maeda, T.; Würthner, F. Halochromic and hydrochromic squaric acid functionalized perylene bisimide. *Chem. Comm.* **2015**, *51*, 7661–7664. [[CrossRef](#)]
12. Pfeifer, D.; Klimant, I.; Borisov, S.M. Ultrabright red-emitting photostable perylene bisimide dyes: New indicators for ratiometric sensing of high pH or carbon dioxide. *Chem. Eur. J.* **2018**, *24*, 10711–10720. [[CrossRef](#)]
13. Yang, L.; Liu, Y.; Li, P.; Liu, Y.L.; Liang, X.M.; Fu, Y.; Ye, F. A dual-mode colorimetric/fluorescent probe based on perylene: Response to acidic pH values. *J. Taiwan Inst. Chem. Eng.* **2021**, *129*, 97–103. [[CrossRef](#)]
14. Zang, L.; Liu, R.C.; Holman, M.W.; Nguyen, K.T.; Adams, D.M. A single-molecule probe based on intramolecular electron transfer. *J. Am. Chem. Soc.* **2002**, *124*, 10640–10641. [[CrossRef](#)] [[PubMed](#)]
15. Ye, F.; Liang, X.M.; Wu, N.; Li, P.; Chai, Q.; Fu, Y. A new perylene-based fluorescent pH chemosensor for strongly acidic condition. *Spectrochim. Acta A Mol. Biomol. Spectrosc.* **2019**, *216*, 359–364. [[CrossRef](#)]
16. Zhang, W.; Gan, S.Y.; Li, F.H.; Han, D.X.; Zhang, Q.X.; Niu, L. pH responding reversible supramolecular self-assembly of water-soluble amino-imidazole-armed perylene diimide dye for biological applications. *RSC Adv.* **2015**, *5*, 2207–2212. [[CrossRef](#)]
17. Li, S.Y.; Long, T.; Wang, Y.; Yang, X.G. Self-assembly, protonation-dependent morphology, and photophysical properties of perylene bisimide with tertiary amine groups. *Dyes Pigm.* **2020**, *173*, 107896. [[CrossRef](#)]
18. Zhang, X.; Rehm, S.; Safont-Sempere, M.M.; Würthner, F. Vesicular perylene dye nanocapsules as supramolecular fluorescent pH sensor systems. *Nature Chem.* **2009**, *1*, 623–629. [[CrossRef](#)] [[PubMed](#)]
19. Pandeeswar, M.; Govindaraju, T. Engineering molecular self-assembly of perylene diimide through pH-responsive chiroptical switching. *Mol. Syst. Des. Eng.* **2016**, *1*, 202–207. [[CrossRef](#)]
20. You, S.S.; Cai, Q.; Müllen, K.; Yang, W.T.; Yin, M.Z. pH-sensitive unimolecular fluorescent polymeric micelles: From volume phase transition to optical response. *Chem. Commun.* **2014**, *50*, 823–825. [[CrossRef](#)]
21. Gao, B.X.; Li, H.X.; Liu, H.M.; Zhang, L.C.; Bai, Q.Q.; Ba, X.W. Water-soluble and fluorescent dendritic perylene bisimides for live-cell imaging. *Chem. Commun.* **2011**, *47*, 3894–3896. [[CrossRef](#)] [[PubMed](#)]

22. Ma, Y.; Zhang, F.; Zhang, J.; Jiang, T.; Li, X.; Wu, J.; Ren, H. A water-soluble fluorescent pH probe based on perylene dyes and its application to cell imaging. *Luminescence* **2016**, *31*, 102–107. [[CrossRef](#)] [[PubMed](#)]
23. Georgiev, N.I.; Said, A.I.; Toshkova, R.A.; Tzoneva, R.D.; Bojinov, V.B. A novel water-soluble perylenetetracarboxylic diimide as a fluorescent pH probe: Chemosensing, biocompatibility and cell imaging. *Dyes Pigm.* **2019**, *160*, 28–36. [[CrossRef](#)]
24. Aigner, D.; Dmitriev, R.I.; Borisov, S.M.; Papkovsky, D.B.; Klimant, I. pH-sensitive perylene bisimide probes for live cell fluorescence lifetime imaging. *J. Mater. Chem. B* **2014**, *2*, 6792–6801. [[CrossRef](#)]
25. Pacheco-Linan, P.J.; Moral, M.; Nueda, M.L.; Cruz-Sanchez, R.; Fernandez-Sainz, J.; Garzon-Ruiz, A.; Bravo, I.; Melguizo, M.; Laborda, J.; Albaladejo, J. Study on the pH dependence of the photophysical properties of a functionalized perylene bisimide and its potential applications as a fluorescence lifetime based pH probe. *J. Phys. Chem. C* **2017**, *121*, 24786–24797. [[CrossRef](#)]
26. Georgiev, N.I.; Sakr, A.R.; Bojinov, V.B. Design and synthesis of novel fluorescence sensing perylene diimides based on photoinduced electron transfer. *Dyes Pigm.* **2011**, *91*, 332–339. [[CrossRef](#)]
27. Daffy, L.M.; Silva, A.P.D.; Gunaratne, H.Q.N.; Huber, C.; Lynch, P.L.M.; Werner, T.; Wolfbeis, O.S. Arenedicarboximide building blocks for fluorescent photoinduced electron transfer pH sensors applicable with different media and communication wavelengths. *Chem. Eur. J.* **1998**, *4*, 1810–1815. [[CrossRef](#)]
28. Golshan, M.; Rostami-Tapeh-Esmail, E.; Salami-Kalajahi, M.; Roghani-Mamaqani, H. A review on synthesis, photophysical properties, and applications of dendrimers with perylene core. *Eur. Polym. J.* **2020**, *137*, 109933. [[CrossRef](#)]
29. Sakr, A.R.; Georgiev, N.I.; Bojinov, V.B. Design, synthesis, and biological activity of perylene tetracarboxydiimide dendrimer. *Synth. Commun.* **2022**, *52*, 2171–2177. [[CrossRef](#)]
30. Wu, J.H.; Peng, M.; Mu, M.X.; Li, J.; Yin, M.Z. Perylene diimide supramolecular aggregates: Constructions and sensing applications. *Supramol. Mater.* **2023**, *2*, 100031. [[CrossRef](#)]
31. Zhang, L.; Zhang, Y.F.; Han, Y.F. A perylene diimide-based fluorescent probe for the selective detection of hypochlorite in living cells. *Mater. Chem. Front.* **2022**, *6*, 2266–2273. [[CrossRef](#)]
32. Ma, L.; Gao, W.J.; Han, X.; Qu, F.L.; Xia, L.; Kong, R.M. A label-free and fluorescence turn-on assay for sensitive detection of hyaluronidase based on hyaluronan-induced perylene self-assembly. *New. J. Chem.* **2019**, *43*, 3383–3389. [[CrossRef](#)]
33. Kar, M.; Anas, M.; Banerjee, P.; Singh, A.; Sen, P.; Mandal, T.K. Amphiphilic perylene bisimide–polymer conjugates by cysteine-based orthogonal strategy: Vesicular aggregation, DNA binding, and cell imaging. *ACS Appl. Polym. Mater.* **2022**, *4*, 3697–3710. [[CrossRef](#)]
34. Zhao, Z.N.; Xu, N.; Wang, Y.; Ling, G.X.; Zhang, P. Perylene diimide-based treatment and diagnosis of diseases. *J. Mater. Chem. B* **2021**, *9*, 8937–8950. [[CrossRef](#)] [[PubMed](#)]
35. Padghan, S.D.; Chung, M.C.; Zhang, Q.S.; Lin, W.C.; Chen, K.Y. 1,6,7-Trisubstituted perylene bisimides with tunable optical properties for colorimetric and “turn-on” fluorescence detection of HCl. *Dyes Pigm.* **2022**, *202*, 110303. [[CrossRef](#)]
36. Hariharan, P.S.; Pitchaimani, J.; Madhu, V.; Anthony, S.P. Perylene diimide based fluorescent dyes for selective sensing of nitroaromatic compounds: Selective sensing in aqueous medium across wide pH range. *J. Fluoresc.* **2016**, *26*, 395–401. [[CrossRef](#)]
37. Zhang, F.X.; Dong, W.Y.; Ma, Y.S.; Jiang, T.Y.; Liu, B.; Li, X.M.; Shao, Y.Y.; Wu, J.S. Fluorescent pH probes for alkaline pH range based on perylene tetra-(alkoxycarbonyl) derivatives. *Arab. J. Chem.* **2020**, *13*, 5900–5910. [[CrossRef](#)]
38. Ding, Y.; Tong, Z.R.; Jin, L.L.; Ye, B.L.; Zhou, J.; Sun, Z.Q.; Yang, H.; Hong, L.J.; Huang, F.H.; Wang, W.L.; et al. An NIR discrete metallacycle constructed from perylene bisimide and tetraphenylethylene fluorophores for imaging-guided cancer radio-chemotherapy. *Adv. Mater.* **2022**, *34*, 2106388. [[CrossRef](#)]
39. Wang, Z.L.; Liu, T.H.; Peng, H.N.; Fang, Y. Advances in molecular design and photophysical engineering of perylene bisimide-containing polyads and multichromophores for film-based fluorescent sensors. *J. Phys. Chem. B* **2023**, *127*, 828–837. [[CrossRef](#)]
40. Lee, Y.L.; Chou, Y.T.; Su, B.K.; Wu, C.C.; Wang, C.H.; Chang, K.H.; Annie Ho, J.; Chou, P.T. Comprehensive thione-derived perylene diimides and their bio-conjugation for simultaneous imaging, tracking, and targeted photodynamic therapy. *J. Am. Chem. Soc.* **2022**, *144*, 17249–17260. [[CrossRef](#)]
41. Kar, M.; Anas, M.; Singh, A.; Basak, A.; Sen, P.; Mandal, T.K. Ion-/thermo-responsive fluorescent perylene-poly(ionic liquid) conjugates: One-pot microwave synthesis, self-aggregation and biological applications. *Eur. Polym. J.* **2022**, *179*, 111561. [[CrossRef](#)]
42. Li, C.W.; Gao, Y.; Huang, R.; Fang, L.; Sun, Y.Y.; Yang, Y.L.; Gou, S.H.; Zhao, J. An effective supramolecular approach to boost the photodynamic therapy efficacy of a near-infrared activating perylene diimide-based photosensitizer. *ACS Mater. Lett.* **2022**, *4*, 657–664. [[CrossRef](#)]
43. Ali, T.H.; Mandal, A.M.; Alhasan, A.; Dehaen, W. Surface fabrication of magnetic core-shell silica nanoparticles with perylene diimide as a fluorescent dye for nucleic acid visualization. *J. Mol. Liq.* **2022**, *359*, 119345.
44. Ding, J.; Sun, M.M.; Liu, J.M.; Liu, X.Q.; Hou, W.L.; Liu, L.; Zhang, H.Q. Colorimetric switching and sensing of CO<sub>2</sub> based on reversible proton movement between the two heavy atoms in low barrier hydrogen bond in PDI radical anion/b-PEI hydrogen bonding complex. *Sens. Actuators B Chem.* **2022**, *372*, 132685. [[CrossRef](#)]
45. Ding, J.; Zhang, J.P.; Wang, H.L.; Zhu, Y.H.; Sun, M.M.; Wang, Q.; Zhang, H.Q. Detecting metal ions by the color change in perylene diimide radical anion/b-PEI complex. *Dyes Pigm.* **2023**, *210*, 110942. [[CrossRef](#)]
46. Kwon, N.Y.; Kim, Y.; Kataria, M.; Park, S.H.; Cho, S.; Harit, A.K.; Woo, H.Y.; Cho, M.J.; Park, M.; Choi, D.H. Donor-σ-acceptor dyad-based polymers for portable sensors: Controlling photoinduced electron transfer via tuning the frontier molecular orbital energies of acceptors. *Macromolecules* **2022**, *55*, 1609–1619. [[CrossRef](#)]

47. Ding, S.; Zhao, S.; Gan, X.Y.; Sun, A.; Xia, Y.; Liu, Y.J. Design of fluorescent hybrid materials based on POSS for sensing applications. *Molecules* **2022**, *27*, 3137. [[CrossRef](#)] [[PubMed](#)]
48. Abumelha, H.M.; Alharbi, H.; Abualnaja, M.M.; Alsharief, H.H.; Ashour, G.R.; Saad, F.A.; El-Metwaly, N.M. Preparation of fluorescent ink using perylene-encapsulated silica nanoparticles toward authentication of documents. *J. Photochem. Photobiol. A Chem.* **2023**, *441*, 114706. [[CrossRef](#)]
49. Qin, J.J.; Wang, H.; Xu, Y.; Shi, F.F.; Yang, S.J.; Huang, H.; Stewar, C.; Li, F.; Han, J.S.; Wu, W. A simple array integrating machine learning for identification of flavonoids in red wines. *RSC Adv.* **2023**, *13*, 8882–8889. [[CrossRef](#)]
50. Kihal, N.; Nazemi, A.; Bourgault, S. Supramolecular nanostructures based on perylene diimide bioconjugates: From self-assembly to applications. *Nanomaterials* **2022**, *12*, 1223. [[CrossRef](#)]
51. Rutschmann, M.; Feldmann, C. Perylene dye@SiO<sub>2</sub> core-shell nanoparticles with intense fluorescence. *J. Mater. Chem. C* **2023**, *11*, 616–621. [[CrossRef](#)]
52. Liu, Q.; Cao, S.F.; Sun, Q.Q.; Xing, C.W.; Gao, W.; Lu, X.Q.; Li, X.Q.; Yang, G.W.; Yu, S.R.; Chen, Y.L. A perylenediimide modified SiO<sub>2</sub>@TiO<sub>2</sub> yolk-shell light-responsive nanozyme: Improved peroxidase-like activity for H<sub>2</sub>O<sub>2</sub> and sarcosine sensing. *J. Hazard. Mater.* **2022**, *436*, 129321. [[CrossRef](#)]
53. Huth, K.; Glaeske, M.; Achazi, K.; Gordeev, G.; Kumar, S.; Arenal, R.; Sharma, S.K.; Adeli, M.; Setaro, A.; Reich, S.; et al. Fluorescent polymer—Single-walled carbon nanotube complexes with charged and noncharged dendronized perylene bisimides for bioimaging studies. *Small* **2018**, *14*, 1800796. [[CrossRef](#)] [[PubMed](#)]
54. Cho, J.; Keum, C.; Lee, S.G.; Lee, S.Y. Aggregation-driven fluorescence quenching of imidazole-functionalized perylene diimide for urea sensing. *Analyst* **2020**, *145*, 7312–7319. [[CrossRef](#)]
55. Liao, C.L.; Zhang, M.; Tian, Q.Y.; Yang, X.M.; Shi, J.; Chen, S.; Che, Y.K.; Wang, C.Y.; Zang, L. Selective turn-on fluorescence detection of formaldehyde in the gas phase. *Sens. Actuators B: Chem.* **2023**, *375*, 132861. [[CrossRef](#)]
56. Guan, W.J.; Zhou, W.J.; Lu, J.; Lu, C. Luminescent films for chemo- and biosensing. *Chem. Soc. Rev.* **2015**, *44*, 6981–7009. [[CrossRef](#)]

**Disclaimer/Publisher's Note:** The statements, opinions and data contained in all publications are solely those of the individual author(s) and contributor(s) and not of MDPI and/or the editor(s). MDPI and/or the editor(s) disclaim responsibility for any injury to people or property resulting from any ideas, methods, instructions or products referred to in the content.